*Physics – Uspekhi* **38** (9) 935 – 964 (1995) 

*REVIEWS OF TOPICAL PROBLEMS* PACS numbers: 36.40.-c; 61.46. + w; 61.66.Bi; 74.70.Wz

# Fullerenes and carbon structures

A V Eletskii, B M Smirnov

## Contents



**Abstract.** A review is given of the current state of research on fullerenes, which are molecules containing 60, 70, 76, 84, etc. carbon atoms arranged on the surface of a sphere or of a spheroid. The structure of fullerenes, the methods for their production, the processes involving them, and the formation of fullerenes in natural gaseous systems are discussed. An analysis is made of the properties of nanotubes and of the methods for generating them. Other carbon compounds resembling fullerenes are considered. The results of the investigations of the behaviour of fullerenes in solutions are given and discussed. The properties of fullerites, which are carbon crystals consisting of fullerenes, and of their compounds are reviewed.

## 1. Introduction

For a long time it has been assumed that carbon can exist in two crystal structures: diamond and graphite [1]. Diamond has the spatial structure in which carbon atoms, forming strong chemical bonds with one another, are oriented relative to one another in three dimensions rather than in a plane. The structure of graphite is layer-like, i.e. each atom forms strong chemical bonds with other atoms located in the same plane, whereas the chemical bonds with the nearest atoms in an adjacent layer are relatively weak. It is therefore considerably easier to separate adjacent layers than to break any one layer.

The tendency of carbon to form surface structures is manifested even more strikingly in new forms of carbon, fullerenes and nanotubes, discovered in the second half of the eighties [2 – 5]. They are closed-surface carbon structures which have special properties as novel materials, as physical objects, and as chemical systems. The development in 1990 of efficient technologies for the synthesis, separation, and deep purification of fullerenes [6, 7] has attracted thousands of researchers to the topic of fullerenes: they include physicists, chemists, materials scientists, and others. Intensive work of these researchers, carried out in hundreds of laboratories in various countries, has led to the discovery of many new interesting properties of fullerenes. These properties make fullerenes not only a new and attractive object for fundamental sciences, but also for a wide range of applications. We shall discuss briefly the interesting physico-chemical properties and potential applications of fullerenes and of systems containing them.

Electric, optical, and mechanical properties of fullerenes in the condensed state are evidence of the rich physical

**A V Eletskii** Russian Scientific Centre 'Kurchatov Institute', pl. Kurchatova 1, 123182 Moscow. Tel. (095) 196 72 80
**B M Smirnov** Institute of High Temperatures, Russian Academy of Sciences, ul. Izhorskaya 13/19, 127412 Moscow. Tel./fax (095) 190 42 22
E-mail: smirnov@termo.msk.su

Received 18 November 1994; revision received 9 March 1995
*Uspekhi Fizicheskikh Nauk* **165** (9) 977 – 1009 (1995)
Translated by A Tybulewicz

content of the phenomena which occur with the participation of fullerenes, as well as of significant chances for finding applications for these materials in electronics, optoelectronics, and other branches of technology. Crystalline fullerenes and films are semiconductors with a band gap of 1.2 – 1.9 eV and they exhibit photoconductivity in the optical range [8 – 11]. Fullerene crystals have relatively low binding energies, so that even at room temperature such crystals undergo phase transitions resulting in orientational disordering and 'unfreezing' of the rotation of the fullerene molecules [12, 13]. Crystals of $C_{60}$, doped with alkali metal atoms, have metallic conduction and become superconducting at temperatures 19 – 33 K, depending on the nature of the alkali metal [14 – 17]. These are record values of the critical temperature for molecular superconductors. Even higher critical temperatures (60 – 100 K) are expected for superconductors based on higher fullerenes [18].

Solutions of fullerenes in organic solvents also have unusual physicochemical properties. For example, the temperature dependence of the solubility of $C_{60}$ in toluene, hexane, and $CS_2$ is nonmonotonic and the solubility maximum occurs at $T = 280$ K [19]. Solutions of fullerenes have nonlinear optical properties, manifested in particular by a strong reduction in the transparency of a solution when the intensity of optical radiation exceeds a certain critical value [20]. This opens up the possibility of using fullerenes in nonlinear optical switches designed to protect optical devices from high-intensity optical radiation.

The discovery of fullerenes has drawn the attention of specialists working on ways of producing synthetic diamonds. The very first experiments [21] demonstrated that a film of $C_{76}$ is an efficient catalyst in the deposition of synthetic diamond coatings from a carbon plasma. The transformation of crystalline fullerene into diamond occurs under much less demanding conditions than in the case of graphite, used traditionally for this purpose. At room temperature, this transformation is observed at a pressure of 20 GPa [22], whereas a corresponding transformation of graphite requires a pressure of 30 – 50 GPa and a temperature of about 900 K [23]. The pressure needed for the conversion of solid fullerene into diamond decreases with increase in temperature. For example, if nickel and cobalt are used as catalysts and fullerene is heated to 1200 – 1850 °C, a pressure of 6.7 GPa is sufficient [24]. The results of recently published experiments [25] on the synthesis of amorphous diamond by shock compression of crystalline fullerene $C_{60}$ look promising. It is important to stress that this synthesis does not require any additional heating of a sample. Hardening of the diamond structure formed in this way, from the temperature which reaches values of the order of 2000 K as a result of shock compression with several tens of gigapascals, is the result of rapid cooling at rates estimated to be $10^{10}$ K $s^{-1}$.

The very first experimental investigations of mechanical properties of fullerenes have confirmed the hope that a very efficient solid lubricant can be made from fullerenes. According to these experiments [26], the surfaces of solids covered by fullerene films have an unusually low coefficient of friction.

A possible revolution in organic chemistry is expected by specialists in this subject. Fullerene molecules, in which the carbon atoms are bound by single or double bonds, are three-dimensional analogues of aromatic structures. They have a high electronegativity and they act as strong oxidants in chemical reactions. The attachment of various chemically different radicals to fullerenes gives rise to a wide class of chemical compounds which have various physicochemical properties. For example, in the recently produced polyfullerene films [27], the $C_{60}$ molecules are not bound by the van der Waals forces (as in a fullerene crystal), but by chemical bonds. These films have plastic properties and represent a new polymer material. The attachment to $C_{60}$ of radicals containing metals belonging to the platinum group [28] maks it possible to produce a ferromagnetic fullerene-based material. New chemical properties have been reported for compounds formed as a result of replacement of some of the carbon atoms in fullerenes with metals. These compounds known as metallocarbohedrenes or met-cars include, for example, $Ti_8C_{12}$, $V_8C_{12}$, $Hf_8C_{12}$, $Zr_8C_{12}$ [29]. Specialists expect much of the results of investigations of physicochemical properties of endohedral compounds of fullerenes [30]. In these compounds, synthesised recently in macroscopic quantities, one or several atoms of a metal or another element are placed inside a spheroidal fullerene structure. The great variety of physicochemical and structural properties of fullerene-based compounds means that we can speak of the chemistry of fullerenes as a new and promising branch of organic chemistry, the development of which may lead to some unexpected results.

Partial thermal decomposition of graphite layers can produce not only fullerene molecules with the closed spherical or spheroidal structure, but also long tiny tubes with their surfaces formed by regular hexagons [4, 5]. These tubes are up to several microns long and their diameters amount to a few nanometres. Depending on the conditions during their manufacture, such 'nanotubes' may consist of one or more layers and can have open or closed ends. The interest in these nanotubes has increased considerably after the development of a technology for their production in gramme quantities [31 – 33]. This interest was stimulated by the results of the first experiments on nanotubes. When an open end of a tube is in contact with the surface of molten lead, the tube becomes filled with lead under the action of the capillary forces and thus becomes a very thin conductor insulated by a shell [34]. High-temperature oxygen treatment produces single-layer tubes with open ends [35, 36]. Experiments on fullerenes and tubes are continuing, and we can count on new surprising discoveries in this field.

Numerous optimistic forecasts are being made of effective commercial use of products based on the fullerene properties. For example, in May 1994 the first large-scale application of fullerenes in electronics was reported [37]. According to this report, which came from Mitsubishi (a large international industrial conglomerate), fullerenes are being used in the manufacture of battery cells. These batteries operate on the basis of the hydrogen attachment reaction and are in many respects similar to the widely used metal hydride nickel batteries, but they are reported to be capable of storing five times more hydrogen. Moreover, these batteries are more efficient and lighter, and they present a lower ecological and health hazard compared with the most advanced (in respect of these properties) lithium batteries.

The $C_{60}$ molecule occupies the central place among fullerenes. It is characterised by the highest symmetry and, consequently, by the highest stability. The structure of this molecule is shown in Figs 1 and 2. This molecule resembles

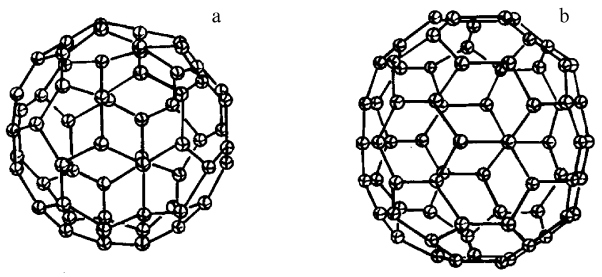


**Figure 1.** Structure of the $C_{60}$ and $C_{70}$ fullerene molecules [366]. In view of its symmetry, all the atoms in the $C_{60}$ molecule are at equivalent positions, whereas in the $C_{70}$ molecule there are five different atomic positions.

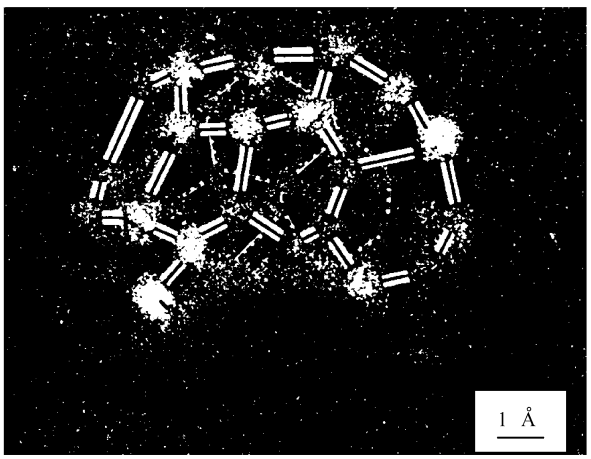


**Figure 2.** Image of the $C_{60}$ structure obtained with the field-ion microscope [80]. The voltage applied to the point was 10.7 kV and the buffer gas (He) pressure was 0.04 Pa.

the cover of a football and has a structure of a regular truncated icosahedron. The carbon atoms are distributed on a spherical surface at the vertices of twenty regular hexagons and twelve regular pentagons, in such a way that each hexagon is in contact with three hexagons and three pentagons, whereas each pentagon is in contact only with hexagons. It therefore follows that each carbon atom in the $C_{60}$ molecule is located at the vertices of two hexagons and one pentagon, and is fundamentally identical with all the other carbon atoms.

The term 'fullerene' originates from the surname of a distinguished American architect, Richard Buckminster-Fuller, who used such structures in the construction of dome-shaped buildings. These buildings resemble the structure of the $C_{60}$ fullerene molecule. In the condensed state, fullerenes are called fullerites, and fullerites doped with metals or other additives are called fullerides.

The problem of the existence of carbon in the form of molecules with a closed surface had been discussed on many occasions in the literature (see Refs [38–43]) well before the first reliable experimental observation of the $C_{60}$ molecule. However, deliberate studies of fullerenes began with the work of Kroto, Heath, O'Brien, Curl, and Smalley [3], who reported detection of the $C_{60}$ molecule as a cluster with a magic number of atoms. This was the stimulus of the investigations of various properties of this cluster [44–50]. These investigations established reliably the closed spherical structure of the $C_{60}$ molecule, which accounts for its high stability. It was also found that the $C_{70}$ molecule, which forms a closed spheroid, is very stable. The fundamental importance of the work of Kroto and his colleagues [3] for the physics of fullerenes was their proposal that the structure of the $C_{60}$ molecule resembles a football. In this structure, the $C_{60}$ system is a molecule and not a cluster, and this is reflected in its principal properties. We shall now discuss these properties in greater detail.

We shall consider the properties of a cluster containing $n$ atoms. The parameters of this cluster, such as the binding energy of an atom being attached, the ionisation potential, the electron affinity energy, the electron excitation energy, the melting point, etc., are not monotonic functions of the number of atoms. These parameters have extrema at what are known as the magic numbers that correspond to the most stable configurations of the atoms in a cluster. In particular, among the most stable configurations are the clusters with filled shells. However, in view of the three-dimensional structure of atoms in a cluster, the parameters of an $A_{2n}$ cluster differ from those of two weakly interacting $A_n$ clusters. This means that the coalescence of two $A_n$ clusters produces an $A_{2n}$ cluster with properties that differ from those of $A_n$.

These arguments do not work in the case of fullerenes since atoms in the fullerene molecules are located on a closed surface. Therefore, the interaction between the atoms in different fullerenes is weaker than between the nearest atoms in one fullerene. It means that the interaction of two fullerene molecules does not result in their coalescence, as in the case of interaction of two clusters with a three-dimensional configuration of atoms. A system of two weakly interacting fullerene molecules is formed and each molecule retains its individual nature. Fullerenes thus represent a special form of carbon which has much in common with graphite, but it differs from both graphite and diamond.

It follows from this discussion that the analogy of the structure of the $C_{60}$ molecule to that of a football, put forward by Kroto et al. [3], was of fundamental importance because this description identified fullerenes as a new form of carbon. In this way the work of Kroto et al. [3] provided the primary stimulus for the study of fullerenes. However, equally important was the relatively simple and efficient technology for the production of fullerenes in macroscopic quantities, put forward and developed in 1990 [6, 51–56]. This technology is based on the conversion of graphite into fullerene and is capable of a production rate of the order of $1\ \mathrm{g\ h^{-1}}$ of $C_{60}$, which is sufficient for extensive investigations. The rate of synthesis of fullerene $C_{70}$ is approximately an order of magnitude less, but $C_{70}$ is produced in sufficient quantities to make possible studies not only of thin films, but also of polycrystalline samples formed from molecules of this kind. Investigations of fullerenes carried out up to 1990 have helped in the development of a technology for their production. The four infrared absorption lines of the $C_{60}$ molecule have served as a 'tracer' in the process of development of this new technology.

One of the powerful stimuli that attracted considerable interest in fullerenes was another hypothesis of Kroto et al. [3], who postulated that the sources of the diffuse near-infrared bands emitted by the interstellar matter are fullerene molecules. The origin of these bands, discovered over 60 years before, is still not clear. The first experiments

designed to determine the absorption spectra of $C_{60}$ in a gas did not confirm this hypothesis. However, later [57] Kroto refined this hypothesis and proposed reasonably that a more probable source of these diffuse bands could be not the $C_{60}$ molecule but the $C_{60}^{+}$ ion, the presence of which in the interstellar matter is more likely. Recently published investigations [58] (see also Ref. [59]) of the infrared absorption spectra of the $C_{60}^{+}$ ion, enclosed in a neon crystalline matrix, appear to confirm this hypothesis.

An important role in the acceleration of research on fullerenes was played by the 1991 discovery of superconductivity, at temperatures below 33 K, of polycrystalline $C_{60}$ doped with alkali metal atoms [14–17, 60–62]. The resultant compounds have at present the highest critical temperatures among molecular superconductors.

Several reviews of the research on fullerenes have been published [63–69]. The present review is based on an earlier one [69], but intensive investigations of the last two years have changed our understanding of the topic. This review aims to describe the current state of research and to analyse the physical picture of the individual properties of fullerene systems.

## 2. Structure of fullerenes

### 2.1 Geometry of the $C_{60}$ molecule

The $C_{60}$ molecule has the structure of a truncated icosahedron. We shall analyse the structure later. The icosahedron is a regular geometric figure whose surface consists of twenty regular triangles [70, 71]. These triangles have twelve shared vertices and twenty shared sides. The icosahedron is the optimal structure for clusters with the pair interaction of atoms, because the structure ensures the maximum number of bonds between the atoms. In particular, fairly small clusters of rare gases have the icosahedron structure. It should be pointed out that, in contrast to fullerenes, a cluster with the icosahedron structure is filled three-dimensionally. For example, the simplest icosahedral cluster contains thirteen atoms with twelve atoms on the surface and one at the centre. Therefore, the geometric figure of the icosahedron does not apply directly to fullerenes. It is the truncated icosahedron that is the model of the $C_{60}$ fullerene molecule.

All the vertices of the icosahedron as a regular figure lie on one sphere, but the radius of the sphere $R$ is somewhat less than the length $L$ of one side of a triangle:

$$R = 0.951L\,. \tag{1}$$

Let us construct the icosahedron as follows. Let us draw a sphere of radius $R$ and pass an axis through the centre of the sphere. The two points of intersection of this axis with the sphere will become vertices of the icosahedron. Next, let us draw two planes perpendicular to the axis separated by a distance $\pm l/2$. If we select $l = 0.851L$, we find that the radius $r$ of the circles formed by intersection of the sphere with the planes is equal to $l$ ($l = r$). Let us inscribe regular pentagons into the circles in such a way that their projections are rotated relative to one another by the angle $\pi/5$. If we connect the nearest points of the figure, the result is the required icosahedron. Each vertex of this figure has five nearest neighbours on the surface and the axis has the fivefold symmetry, i.e. rotation about this axis by the angle $2\pi/5$ conserves the figure. The icosahedron has six such symmetry axes passing through the centre and opposite vertices of the figure. Ten more symmetry axes of the icosahedron are perpendicular to the planes of the triangles (they pass through the centre of the figure and through the centres of the opposite triangles). Since rotation about any of these ten axes by the angle $2\pi/3$ conserves the figure, they are threefold axes.

Let us now go over from the icosahedron to the truncated form which models the $C_{60}$ fullerene molecule. We shall do this by drawing a new sphere with its centre at the centre of the icosahedron in such a way that it intersects each side of the icosahedron into three equal parts. The points of intersection are the vertices of the new figure. The number of these intersection points is twice the number of the icosahedron sides, i.e. there are sixty such points. The truncated icosahedron is obtained by joining the nearest vertices. Each vertex of this figure has three nearest neighbours. The above operation can be carried out in a different way. We can separate each side of the initial icosahedron into three equal parts and connect the nearest vertices. In this way, a regular pentagonal pyramid is cut off from each icosahedron vertex. The base of this pyramid is a regular pentagon. This operation transforms each regular triangle of the icosahedron surface into a regular hexagon on the surface of the truncated icosahedron. The side $a$ of the latter is one-third of the side of the initial triangle ($a = L/3$). This operation therefore cuts off twelve regular pentagonal pyramids from the icosahedron and the surface of the resultant figure includes twelve regular pentagons and twenty regular hexagons. All ninety sides of the truncated icosahedron have the same length $a$.

We shall use $R'$ to denote the radius of the sphere, the surface of which contains all the vertices of the truncated icosahedron. We shall use $h$ for the distance from the centre of this sphere to the centre of a hexagon (or a triangle in the initial icosahedron) and $h'$ for the distance from the centre of the sphere to the centres of the pentagons. These quantities are related as follows:

$$R' = 2.478a, \tag{2}$$

$$h = 2.267a, \tag{3}$$

$$h' = 2.327a. \tag{4}$$

Moreover, it follows from formula (1) that the relationship between the radius of the initial icosahedron and the long side of the truncated icosahedron is

$$R = 2.853a. \tag{5}$$

The above relationships will be useful in the analysis of the structure of the $C_{60}$ fullerene molecule.

We must stress the high symmetry of the figures discussed above. Both the icosahedron and its truncated form, the latter modelling the $C_{60}$ fullerene molecule, have ten threefold symmetry axes. This means that the rotation about these axes by the angle $2\pi/3$ conserves the figures. The threefold axes pass through the centre of the figure and the centres of the surface triangles in the case of the icosahedron or through the centre of the figure and through the centres of the surface hexagons of the truncated icosahedron. Moreover, both icosahedra have six fivefold symmetry axes. In the case of the icosahedron, these axes pass through the centre of the figure and through its vertices, whereas in the truncated icosahedron they join the centre of the figure to the centres of the surface pentagons.

## 2.2 Structure of fullerenes

The $s^2p^2$ electron shell of the carbon atom ensures the optimal structure of carbon when the neighbouring atoms form pentagons and hexagons. Such a structure occurs also in the most common natural modifications of solid carbon: diamond and graphite. This structure is optimal also for the most stable carbon clusters formed as a result of thermal evaporation of graphite. Stable carbon molecules form a closed surface on which the carbon atoms are located. This closed surface consists of hexagons and pentagons. A hexagon with carbon atoms at its vertices is a structure component of fullerenes and of graphite. Since the most efficient methods for the production of fullerenes are based on thermal decomposition of graphite, it is natural to assume that the hexagons forming the spherical or spheroidal surface of the fullerene molecules have the same dimensions as the hexagons in graphite. We shall use this analogy in the subsequent analysis of the $C_{60}$ structure.

Graphite consists of layers which are formed by regular hexagons with the 0.142 nm side and separated by distances of 0.335 nm [74]. The atoms in the adjacent layers are not located one above the other, but are shifted by half the lattice constant. We shall calculate the radius of the $C_{60}$ fullerene molecule on the assumption that it is composed of the same hexagons as graphite. If we use the truncated icosahedron model for the $C_{60}$ molecule, we find that the radius of a molecule calculated from formula (2) is $R = 2.48a = 0.35$ nm, where $a$ is the distance between the nearest neighbours.

In modelling the $C_{60}$ molecule by the truncated icosahedron we have assumed above that all the bonds in the fullerene molecule are equivalent. Consequently, according to this model, they have the same length, which is equal to the bond length in a graphite layer. In reality, the $C_{60}$ structure comprises two types of bond: one of which (double) is a shared side of two hexagons and the other (single) is a shared side of a pentagon and a hexagon. The results of various experiments [75–77] have shown that the lengths of these bonds are $0.139 \pm 0.001$ and $0.144 \pm 0.001$ nm, respectively. Therefore, the hexagons forming the $C_{60}$ structure are slightly irregular and the above estimate of the dimensions of fullerene is accurate to within 1% –2%. A more accurate value of the radius of the $C_{60}$ molecule, deduced from x-ray structure analysis [55], is 0.357 nm. All the carbon atoms in the $C_{60}$ molecule are at equivalent positions, so that each atom belongs simultaneously to two hexagons and one pentagon. This is confirmed by the nature of the NMR spectrum of the $C_{60}$ molecule containing the $^{13}C$ isotope. In the case of pure $C_{60}$, this spectrum has only one resonant feature.

The common structure components of graphite and of the $C_{60}$ fullerene molecule determine the nature of the process of formation of fullerenes by decomposition of graphite. Moderate heating of graphite breaks the bonds between the separate layers and an evaporated layer then splits into separate fragments. These fragments are combinations of hexagons and one of them is then used to form a cluster. We can propose a variety of methods for assembling a fullerene molecule from such fragments (Fig. 3). It would seem that the $C_{60}$ molecule can be constructed more simply from ten hexagons containing sixty atoms, combining them to form a closed structure. However, this requires cutting of some hexagons. Since a closed surface cannot be constructed solely of hexagons, it follows that the fragments from which the $C_{60}$ molecule is assembled should be of smaller size. For example, this molecule can be assembled from six independent double hexagons, each of which contains ten atoms. This is clearly the simplest method for assembling the $C_{60}$ fullerene molecule. This method may be modified if we form a molecule from the fragments that contain double hexagons. In particular, Fig. 3a shows one such fragment. A possible way of synthesising the $C_{60}$ molecule from two such fragments is illustrated in Fig. 3b. This fullerene assembly mechanism was proposed by us earlier [68]. The approach was developed further subsequently [367].

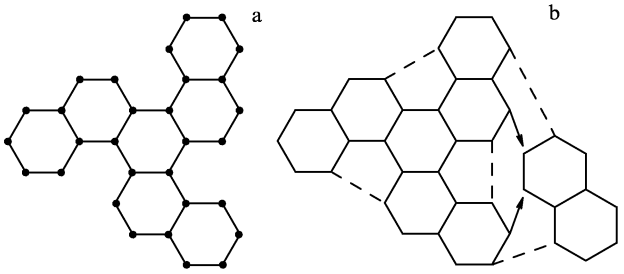


**Figure 3.** Possible ways of synthesising the $C_{60}$ molecule from graphite fragments [68, 69]. (a) Graphite fragment which can be the basis for the synthesis of half of the $C_{60}$ fullerene. (b) Possible formation of a part of a closed carbon cluster from graphite fragments. Coalescence of two fragments is shown. The larger fragment, consisting of seven hexagons (thirty atoms) is twisted to form a three-dimensional structure so that the dashed lines close the relevant sides of a pentagon. Next, the fragment consisting of two hexagons (ten atoms) forms, with the larger fragment, a hexagon (closed by arrows) and two pentagons (closed by dashed lines). In this way the two fragments form a part of a $C_{60}$ cluster containing forty atoms and including six closed pentagons and ten closed hexagons. The $C_{60}$ fullerene can be formed from this fragment by adding two more fragments which are double hexagons.

Direct observations of the fullerene structure have become possible as a result of constructions and improvements in the field-ion microscope [78, 79]. This instrument makes it possible to locate spatially the positions of the separate atoms forming a molecule by field ionisation of atoms of a buffer gas in a strongly inhomogeneous electric field near the investigated molecule. Fig. 2 shows an image of the $C_{60}$ molecule obtained in this way [80]. The buffer gas used was helium at a pressure of $4 \times 10^{-2}$ Pa.

The $C_{70}$ molecule (Figs 1 and 4) is formed from $C_{60}$ by introducing a belt of ten carbon atoms in the equatorial

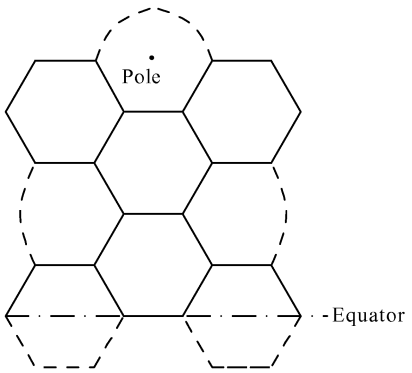


**Figure 4.** Structure and bonds in the $C_{70}$ molecule.

**Table 1.** Characteristics of various types of C–C bonds in the $C_{70}$ molecules [81].

| Bond No. | Number of bonds of given type | Type of bonds | Bond length/nm |
|---|---|---|---|
| 1 | 5 | hexagon – hexagon | $0.141^{+0.003}_{-0.001}$ |
| 2 | 20 | hexagon – hexagon | 0.139±0.001 |
| 3 | 10 | hexagon – pentagon | $0.147^{+0.001}_{-0.003}$ |
| 4 | 20 | hexagon – pentagon | 0.146±0.001 |
| 5 | 10 | hexagon – hexagon | 0.137±0.001 |
| 6 | 20 | hexagon – pentagon | 0.147±0.001 |
| 7 | 10 | hexagon – hexagon | 0.137±0.001 |
| 8 | 10 | hexagon – pentagon | 0.1464±0.0009 |

part of the sphere and stretching this part. This representation of the $C_{70}$ structure agrees, in particular, with the nature of the NMR spectrum of this molecule, which — in contrast to the spectrum of $C_{60}$ — consists of five peaks. The geometric parameters of the $C_{70}$ molecule have been reconstructed from measurements of the electron energy loss spectrum when electrons are scattered elastically by the $C_{70}$ molecules in a gaseous state [81]. The total number of bonds between atoms in this molecule is 105 and among them there are eight groups of different bonds, which are identified in Fig. 4; the lengths of these bonds are listed in Table 1. It follows from Table 1 that the lengths of the bonds labelled 3, 4, 6, and 8 in Fig. 4 are close to 0.146 nm. These bonds lie on the boundary between a pentagon and a hexagon, and they join two hexagons. Bonds 5 and 7 are located at a boundary between two hexagons and join two pentagons. The length of these bonds is close to 0.137 nm. Bonds 1 and 2 are at a boundary between two hexagons and they join two hexagons. The length of these bonds is approximately 0.14 nm and they are of similar nature to the bonds between the nearest carbon atoms in graphite (of length 0.142 nm). Thus, although the $C_{70}$ molecule has eight different types of bonds, characterised by specific symmetries in the molecule, in the first approximation all these bonds can be reduced to three groups in accordance with the nature of the figures which they separate or link. In this approximation we have three bond lengths for the $C_{70}$ molecule. A bond of type 1, undistorted by the proximity of pentagons, is similar to the C–C bond in a graphite layer. The length of this bond, 0.141 + 0.003 (−0.001) nm, is practically identical with the corresponding bond length in graphite (0.142 nm). A bond of type 2, joining the vertices of a pentagon and a hexagon in the equatorial region of $C_{70}$, is $0.139 \pm 0.001$ nm long, i. e. it is intermediate between the lengths of the bonds joining the vertices of two hexagons and five pentagons, respectively.

The total height of the $C_{70}$ molecule, defined as the distance between the pentagonal faces located in two mutually opposite polar regions, is $0.780 \pm 0.001$ nm for a molecule at rest. The diameter of the equatorial circle, passing through the centres of the carbon atoms, is $0.694 \pm 0.005$ nm. A comparison of this value with the diameter of the circle ($0.699 \pm 0.005$ nm) passing through the centres of those atoms which are joined by type 3 bonds, i. e. the comparison with the diameter of the circle separated by one layer from the equatorial plane, indicates — according to the authors of Ref. [81] — that the structure of the $C_{70}$ molecule has a waist in the equatorial plane, but — within the limits of precision of the results — this conclusion is not reliable.

The symmetry of the $C_{70}$ molecule is lower than that of $C_{60}$. If we assume that the atoms of the former are on the surface of an ellipsoid of revolution and that the polar caps are formed by pentagons perpendicular to a symmetry plane, we find that the $C_{70}$ molecule has one fivefold symmetry axis which coincides with the major axis of the ellipsoid. This symmetry axis should be supplemented by a mirror plane, perpendicular to the axis and passing through the centre of the figure, and also by an inversion symmetry, which follows from the other symmetry characteristics.

The symmetry of the $C_{76}$ fullerene molecule (Fig. 5) is even lower than that of the $C_{70}$ molecule. The NMR spectrum of the $C_{76}$ molecule contains nineteen different lines of approximately the same intensity [82]. Hence, the carbon atoms in the $C_{76}$ molecule can occupy nineteen different positions and each of these nineteen groups consists of four atoms. The surface of the $C_{76}$ molecule is covered by twelve pentagons and twenty-eight hexagons. Such a molecule can be formed if two $C_{60}$ 'polar caps', representing pentagons surrounded by hexagons, are encircled alternately by pentagons and hexagons and these are joined together in such a way that pentagons are prevented from contact with one another by hexagons. A closed structure is formed by the addition of another pair of pentagons and a pair of hexagons. Fig. 5 shows the structure of the $C_{76}$ molecule, oriented perpendicular to each of the three symmetry axes of the molecule [82]. The dimensions of the $C_{76}$ molecule along the directions of all its symmetry axes are 0.879, 0.764, and 0.668 nm, respectively.

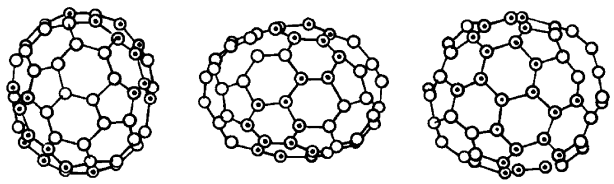

**Figure 5.** Structure of the $C_{76}$ molecule, oriented perpendicular to each of its three symmetry axes. Symbols (circles) represent different positions of atoms in the structure [82].

Additional information on the carbon structures can be obtained from an analysis of the mobility of charged carbon clusters $C_n^+$, measured for clusters of different sizes [83 – 86]. It is evident from Fig. 6 that there are several families of such dependences, so that the same cluster size $n$ may correspond to several mobility values. This is evidence of the existence of several isomeric forms of the $C_n$ clusters, which correspond also to different mobilities for the same value of $n$. Hence, we can distinguish different families of the structures of carbon ion clusters in accordance with their mobilities. The monotonic nature of each of the mobility dependences indicates a continuous change in the size of a cluster of a given type as the number of atoms in it increases. For example, the black dots joined by curve *1* correspond to a linear structure of a $C_n^+$ cluster. This structure is realised for $3 \leqslant n \leqslant 10$. Curve *2*, based on the results of an analysis of Ref. [83], represents clusters with a closed planar structure, which is realised for $6 \leqslant n \leqslant 36$. Naturally, the mobility of a $C_n^+$ isomer, which has a closed cyclic structure, exceeds the mobility of a cluster with a linear structure and the same number of atoms. Curve *3*, representing clusters with

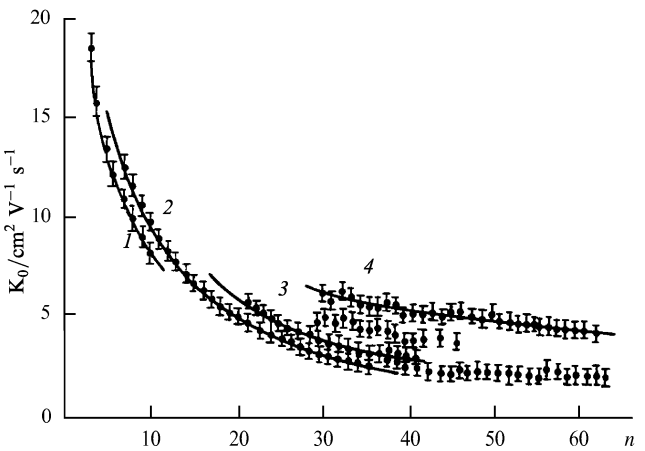


**Figure 6.** Dependence of the mobility of $C_n^+$ clusters in He on their size $n$ [83–86]. The mobility values are reduced to normal conditions.

$21 \leqslant n \leqslant 61$, is very close to curve *2*. It is attributed in Ref. [83] to a closed planar structure of a cluster containing two cyclic configurations. Curve *4*, representing clusters with $30 \leqslant n \leqslant 61$, is attributed to fullerenes and clusters with a closed three-dimensional structure. This follows from the value of the mobility of these clusters, which is considerably higher than the mobility of clusters with the same number of atoms and a planar structure. Therefore, clusters represented by curve *4* should be most compact. Fig. 6 includes also the mobility of a $C_{60}^+$ cluster, which more or less fits curve *4*. The dependences discussed above apply also to negative carbon ions.

### 2.3 Structure of metallo-carbohedrenes

Fullerenes form a whole class of carbon molecules in which atoms are on a closed surface. The carbon atoms in such cluster molecules form hexagons and pentagons and, according to the Euler theorem, a closed surface is formed when each of these figures contains twelve pentagons, whereas the number of hexagons can vary. Since each surface atom has three nearest neighbours, the relationship between the number of atoms $n$ in a fullerene molecule and the number of surface hexagons $m$ is

$$n = 20 + 2m\,.$$

Hence, in particular, it follows that the $C_{60}$, $C_{70}$, $C_{76}$, and $C_{84}$ fullerene molecules contain respectively 20, 25, 28, and 32 surface hexagons. The simplest of the possible structures, which has no hexagons, contains twenty carbon atoms. The surface of this $C_{20}$ molecule is formed by twelve pentagons with all their vertices located on a sphere.

A simple method of forming this structure is as follows. Let us place twenty atoms at the vertices of four pentagons whose planes are parallel and whose vertices are located on the surface of a sphere. The sides of the upper and lower pentagons are $a$, which is the distance between the nearest neighbours in the figure; the sides of the other two pentagons amount to $2a\sin(\pi/5) = 1.661a$. Since all the vertices of the pentagons lie on a sphere, it means that the distance from the centre to the planes of the large pentagons is $0.263a$ and the distance to the planes of the small pentagons is $1.174a$. The corresponding radii of the circles, which are sections of the sphere into which the pentagons are inscribed, amount to $0.851a$ and $1.376a$. The radius of the sphere on which the pentagon vertices are located is $1.401a$.

As pointed out earlier, if the nearest vertices of the pentagons lying on the surface of a sphere are joined, the result is the surface of a figure consisting of twelve regular pentagons. This figure, like the icosahedron, is characterised by six fivefold symmetry axes which pass through the centre of the figure and through the centres of the surface pentagons, as well as ten threefold axes passing through the centre and through the vertices of the figure. Rotation about these axes by the angle $2\pi/3$ ensures that the edges emerging from the vertices of the figure located on the axis are transformed into each other. We can see that the resultant figure has a high symmetry.

In view of its high symmetry, this $C_{20}$ molecule should have a high binding energy and should be more stable than the molecules and structures in which the number of atoms differs slightly from twenty. However, it is problematic whether such a molecule can be assembled. In fact, in the case of the $C_{60}$ molecule some components of this molecule existed at the beginning. Such components could have been formed by splitting of a graphite plane into separate fragments consisting of hexagons, which might be joined to form such molecules. Since the $C_{20}$ molecule does not contain hexagons, it has to be assembled from separate atoms, which is the reason why the formation of the $C_{20}$ molecule in reality is open to question.

Although the $C_{20}$ fullerene structure described above has not been realised in practice, Castleman and his colleagues at the Pennsylvania State University [29, 87, 88] synthesised structures of the $M_8C_{12}$ type, similar to this fullerene; here M is a metal atom. These molecules are analogues of the simplest fullerenes. The general experimental setup [87–90] involved the formation of an ionised beam of a metal vapour formed by irradiation of a metal surface with a focused laser beam. A metal plasma beam produced in this way was mixed with a stream of helium carrying hydrocarbons, such as methane, ethylene, acetylene, propylene, and benzene. In each case the mass spectrum of the products of such a process had a sharp peak corresponding to the compound $M_8C_{12}$. The metal was one of the transition group, such as Ti, V, Hf, or Zr. The resultant compounds were classified as metallo-carbohedrenes or, briefly, met-cars. The metallo-carbohedrene molecules are more stable than other compounds of carbon with a metal [91–94]. In addition to neutral met-cars, it was found that stable negative and positive ions of these molecules were formed in a mixture of ionised gases and these molecules were detected by mass spectrometry.

The bonds of the atoms in metallo-carbohedrene molecules are strong, For example, the binding energy per one atom in the $Ti_8C_{12}$ molecule is 6.1 eV [91, 92]. For comparison, one should mention that the same energy for the $C_{60}$ fullerene molecule is 7.4–7.6 eV [93, 94]. The structure of the $C_{20}$ simplest fullerene is the dodecahedron. This is a figure in which all the atoms are located on a sphere and the surface of this sphere, formed by joining the nearest atoms, consists of twelve regular pentagons. In an analysis of the structure of the metallo-carbohedrene molecules (Fig. 7), it is necessary to identify the dodecahedron symmetry, which is maintained in these compounds. Let us separate eight out of the twenty dodecahedron atoms in such a way that none of the pairs of these atoms forms a bond, i. e. that none of the pairs is joined to the side of the

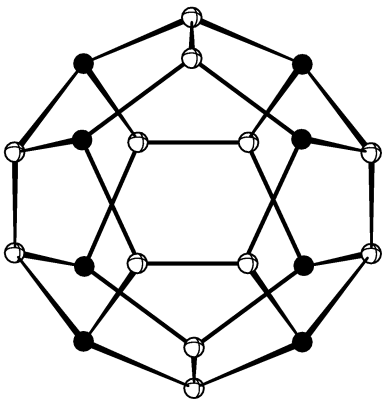

**Figure 7.** Structure of the $Ti_8C_{12}$ molecule [91]. Titanium is represented by black dots and carbon by open circles.

pentagon lying on the surface of the figure. Then these atoms form a cube and the cube contains two nonneighbouring atoms of the pentagons on the dodecahedron surface. We shall call these the metal atoms and the others the carbon atoms. Then the carbon atoms in this structure form the $C_2$ molecules, which are located above the corresponding cube planes, so that their axes are parallel to the cube planes and the projections divide these planes into halves. Such a molecular structure is retained after its subsequent transformation which involves a change in the length of the cube edge and a change in the length of the bond in the carbon molecule. A simultaneous similar transformation of the size of the molecule is also possible. In the $C_{20}$ fullerene molecule each carbon atom has three nearest neighbours, but in metallo-carbohedrene molecules each metal atom has three carbon atoms as neighbours and in the case of each carbon atom the neighbours are two metal and one carbon atoms. Moreover, all the carbon atoms, like all the metal atoms, occupy identical positions in the molecule. This is evidence of the high symmetry of the metallo-carbohedrene molecules.

This method of constructing a metallo-carbohedrene-molecule makes it possible to identify its symmetry, which is also the additional symmetry for the $C_{20}$ molecule. Let us represent a metallo-carbohedrene molecule by a large cube with atoms that are not the nearest neighbours at its vertices. Then, above each of the surface squares of the cube let us place one $C_2$ molecule with its centre located above the centre of the square and its axis parallel to the sides of the square. The axes of the molecules located above the adjacent cube faces are mutually perpendicular. In this way the surfaces of metallo-carbohedrenes are formed by three mirror symmetry planes which pass through the centre of the figure and are parallel to the surface squares of the cube. Mirror reflection of the figure relative to these planes (and corresponding inversion relative to the centre) conserve the figure. This symmetry is additional for the $C_{20}$ fullerene molecule and it is conserved in transformations which convert this molecule into metallo-carbohedrenes. Such a symmetry testifies to the stability of the metallo-carbohedrene molecules.

Let us denote the length of the bond between two carbon atoms by $a$, the length of the metal–carbon bond by $b$, and the distance between two metal atoms, i. e. the length of the side of a cube, by $c$. On the basis of this structure of a metallo-carbohedrene molecule we obtain the following relationship between these three parameters:

$$b^2 \geqslant \frac{1}{4}(c-a)^2 + \frac{1}{4}c^2 , \qquad (6)$$

where the sign of equality in the above expression corresponds to the case when the carbon molecules are located on the cube planes. Calculations [91] show that the distance between the metal atoms in the $Ti_8C_{12}$ metallo-carbohedrene molecule is approximately twice the length of the bond between two carbon atoms and the metal–carbon bond length is approximately 30% greater than the length of the carbon bond. Such a structure can be formed from the dodecahedron if the length of the bonds between the adjacent carbon atoms is reduced by 20% . The structure of the $Ti_8C_{12}$ molecule obtained in this way is shown in Fig. 7 [91]. Other metallo-carbohedrene molecules have a similar structure.

It follows that metallo-carbohedrenes represent a new class of chemical compounds and their structure is similar to that of fullerenes. These compounds form quite readily in an ionised mixture and are therefore of both scientific and practical interest.

## 3. Production of fullerenes

### 3.1 Formation of $C_{60}$ molecules

The most efficient method for the production of fullerenes is based on thermal decompostion of graphite in accordance with the procedure for assembly of a fullerene molecule discussed above. The optimal conditions for the formation of fullerene molecules are achieved by moderate heating of graphite so that the products of its decomposition consist of fragments which are components of the fullerene molecular structure. The bonds between separate graphite layers should be destroyed but the evaporated carbon should not be split into separate atoms. Under these conditions the evaporated graphite consists of fragments which contain hexagonal configurations of the carbon atoms. It is these fragments that are used to assemble the $C_{60}$ and other fullerene molecules.

Graphite can be decomposed by electric heating of a graphite electrode [54] or by laser irradiation of a graphite surface [52]. These processes take place in a buffer gas, which is usually helium. The main role of helium is obviously to cool the fragments which have a high degree of the vibrational excitation preventing their coalescence into stable structures. Moreover, helium atoms carry away the energy released as a result of such coalescence. The advantage of helium over other buffer gases is related to the high efficiency of quenching of vibrationally excited molecules. There is obviously an optimal buffer gas pressure, because at higher pressures the aggregation of the carbon fragments is hindered. Experience shows that the optimal helium pressure is in the range 50–100 Torr.

The most convenient and widely used method for extracting fullerenes from the products of thermal decomposition of graphite (soot containing fullerenes), followed by their separation and purification, is based on the use of solvents and sorbents. This method, first implemented in an investigation reported in Refs [6, 54–56], consists of several stages. In the first stage, soot containing fullerenes is treated in a nonpolar solvent, which can be benzene, toluene, or other substances. Fullerenes are quite soluble in

these solvents and are separated from the insoluble fraction, which usually amounts to 70% –80% of the phase containing fullerenes. A typical solubility of fullerenes in solutions used in their synthesis amounts to a few tenths of a molar percent. Quantitative data on the solubility of fullerenes in various solvents are given in Table 4.

Evaporation of a fullerene solution formed in this way produces a black polycrystalline powder which is a mixture of fullerenes of different types. A typical mass spectrum of such a product [6] shows that the fullerene extract represents 80% – 90% of $C_{60}$ and 10% – 15% of $C_{70}$. Moreover, there is a small amount (representing a fraction of a percent) of higher fullerenes, which are quite difficult to extract.

The separation of the fullerenes from such an extract is based on the concepts of liquid chromatography. A fullerene extract, dissolved in one of the solvents, is passed through a sorbent which may be aluminium, activated carbon, or some other material with high sorption characteristics. Fullerenes are sorbed by one of these materials and then extracted with the help of a pure solvent. The extraction efficiency is governed by the sorbent – fullerene – solvent combination and usually depends — for a given sorbent and solvent — on the type of fullerene [95]. Therefore, the solvent passed through a sorbent with fullerenes sorbed by it extracts consecutively fullerenes of different kinds from the sorbent, so that the fullerenes can then be readily separated.

Further development of this technology of production, separation, and purification of fullerenes — based on electric-arc synthesis of soot containing fullerenes and the subsequent separation of fullerenes by sorbents and solvents [6, 54 – 56] — has led to the manufacture of equipment capable of synthesising $C_{60}$ at a rate of the order of 1 g per hour [7, 96]. By way of example, let us consider the apparatus for the production of fullerenes described in Ref. [7]. A chamber consists of a water-cooled jacket in the form of a cylinder containing a graphite electrode vapour. One of these electrodes is a flat disk and the other is a sharpened rod, which is pressed against the disk by a soft spring. An arc discharge is struck between these two electrodes and it causes sputtering of the rod. The spring tension is varied in such a way so that the bulk of the power supplied to the system is released in the arc and not in the rod. The chamber is filled with helium at a pressure of the order of 100 Torr. The discharge parameters are as follows: the alternating current is 100 – 200 A and the voltage across the electrodes is 10 – 20 V. The discharge ensures that the rate of evaporation of the graphite rod is of the order of 10 g $h^{-1}$. After several hours of such arc burning, the internal surface of the water-cooled copper jacket is covered by carbon soot, which is carefully scraped off from the surface and within about three hours is subjected to the action of boiling toluene. The resultant dark brown liquid is evaporated in a rotating vessel. This produces a black powder whose weight is about 10% of the original carbon soot. A spectroscopic analysis shows that this powder consists almost completely of the $C_{60}$ and $C_{70}$ fullerenes in the ratio of about 10 : 1. Therefore, the technology described here makes it possible to produce the $C_{60}$ and $C_{70}$ fullerenes in gramme quantities.

Changes in the parameters of this process and in the configuration of the apparatus can alter the efficiency of the process and the composition of the product. For example, some modernisation of the technology described above [97] has made it possible to obtain a carbon condensate which can be separated from a toluene solution to produce almost pure $C_{60}$ without significant amounts of other fullerenes. In this case the electrodes are two finely sharpened graphite rods facing one another with the sharp points. The power consumption is lower (voltages 5 – 8 V, currents 100 – 180 A) and the helium pressure is higher (180 Torr). The rate of production of pure $C_{60}$ in this apparatus is about 50 mg $h^{-1}$. The high quality of the product is confirmed by mass spectrometry and by NMR measurements.

### 3.2 Production of higher fullerenes

An electric-arc discharge is sufficient for the production of pure $C_{60}$, but the formation of higher fullerenes requires a fairly complex extraction procedure based on liquid chromatography [98]. This method makes it possible not only to separate $C_{60}$ from $C_{70}$ [98], but also to accumulate the rarer fullerenes $C_{76}$, $C_{84}$, $C_{90}$, and $C_{94}$. These processes occur in parallel with the formation of $C_{60}$, the separation of which makes it possible to enrich the mixture with higher fullerenes. For example, it was reported in Ref. [99] that a carbon deposit, formed by thermal evaporation of a graphite electrode in an electric arc, yielded pure $C_{60}$ when a deposit was treated with a mixture of hexane with toluene in the ratio 95 : 5. This led to washing out and subsequent extraction of pure $C_{60}$. An increase in the amount of toluene in the solution to 50% made it possible to extract pure $C_{70}$ and a further increase in the proportion of toluene yielded four yellowish fractions. A repeated chromatography of these fractions on an aluminium surface made it possible to prepare fairly pure fullerenes $C_{76}$, $C_{84}$, $C_{90}$, and $C_{94}$. Treatment of the first of these fractions, adsorbed on an aluminium surface, with a mixture of hexane with toluene in the ratio 95 : 5 led to complete dissolution of the $C_{70}$ molecules in a mixture. The remaining yellowish condensate consisted almost totally of the $C_{76}$ molecules, as confirmed by the results of a liquid chromatographic analysis.

It follows that high-pressure liquid chromatography is a reliable method for the production of higher fullerenes. The content of the higher fullerenes $C_{76}$, $C_{84}$, $C_{90}$, and $C_{94}$ by weight in the initial carbon deposit, used to prepare $C_{60}$ and $C_{70}$, does not exceed 3% – 4%. This method makes it possible to wash out the fullerenes $C_{60}$ and $C_{70}$ from the condensate and thus obtain an extract containing higher fullerenes of certain compositions in milligramme quantities. The subsequent modernisation of the chromatographic fullerene separation method, based on distillation of a solution of soot containing fullerenes under solvent-boiling conditions [100, 101], reduces by an order of magnitude the solvent consumption and increases similarly the degree of purification of fullerenes.

In spite of the obvious success of the chromatographic technology of fullerene separation and purification, the problem of production of higher fullerenes in macroscopic quantities sufficient for complete and comprehensive investigation of their properties in the condensed state is far from fully solved. The productivity of the best chromatographic equipment does not exceed a few milligrammes per hour, which is obviously insufficient for research requirements. The cost of higher fullerenes ($C_{76}$, $C_{84}$) in the world market is thousands of dollars per gramme, so that these fullerenes are not readily available for scientific research. The intensive search for new and less costly methods for producing higher fullerenes is continuing. Promising results were obtained recently [102] in an

attempt to combine the electric-arc and liquid stages of the production of higher fullerenes. A solution of fullerenes in toluene or benzene was obtained by a dc discharge in an arc with graphite electrodes immersed in a suitable solvent. The subsequent mass-spectroscopic analysis showed that the solution was filled with $C_n$ clusters in which the number of atoms ranged from 4 to 76. It was of considerable interest that, in contrast to the mass spectrum obtained after electrothermal decomposition of graphite in a helium atmosphere, the $C_{60}$ fullerene did not dominate the mass spectrum of the product obtained in this way. The $C_{50}$ clusters were present in the highest concentration: their amount exceeded by a factor of 3 – 8 the amount of the $C_{60}$ fullerene. The concentration of the higher fullerenes with $n > 60$ was of the same magnitude as that of $C_{60}$. This approach promises a reduction in the cost and time of production of fullerenes higher than $C_{60}$.

Graphite is the most appropriate material for the production of fullerenes because its structure has much in common with the structure of fullerenes. Nevertheless, fullerenes can be prepared also from other carbon materials. One example is the use of a liquid-crystal mesophase [103], formed by pyrolysis of a number of carbon compounds at temperatures 370 – 500 °C [104], as the source of $C_{60}$. This liquid-crystal mesophase [103] is a resinous substance, representing the product of continuous hydrogenation of brown coal at a hydrogen pressure of $\sim$100 bar for 2.5 h. Removal of the volatile fragments at 400 °C in a low-pressure chamber produces a mesophase with 0.82 aromaticity: the composition of this phase is 92.7% C, 4.8% H, 1% N, and 1.5% O. Laser irradiation of the surface of the mesophase produces a volatile fraction with a high $C_{60}$ content. It is obvious that the pyrolysis of coals and of carbon compounds is one of the promising directions for the production of fullerenes.

Another instructive example of a nontraditional approach to the task of production of fullerenes is a recent paper of Taylor et al. [105]. It is reported there that efficient synthesis of $C_{60}$ is possible as a result of pyrolysis of naphthalene in a silicon tube, heated by a propane burner to $T \approx 1300$ K. A mass-spectroscopic analysis of the products of pyrolysis is evidence of a considerable content (of the order of 1%) of the $C_{60}$ fullerene. Moreover, an investigation of the mass spectrum of the products of pyrolysis makes it possible to reconstruct the mechanism of the synthesis of $C_{60}$ and other fullerenes. The naphthalene molecule, $C_{10}H_8$, consists of two aromatic carbon rings and, as demonstrated by us earlier [68, 69], can serve as a ready-made component for the synthesis of the $C_{60}$ molecule. The methods for the synthesis of the $C_{60}$ molecule from double aromatic $C_{10}$ rings are presented in Fig. 3. It follows from a mass-spectrometric analysis of the products of pyrolysis of naphthalene [105] that the products include all the intermediate stages of the assembly of $C_{60}$ from $C_{10}$ shown in Fig. 3. This is a direct experimental proof of the mechanism of the synthesis of $C_{60}$ from $C_{10}$ components proposed in Refs [68, 69]. More detailed reviews of the latest progress in the technology of the production of fullerenes can be found in Refs [106, 107].

### 3.3 Methods for the purification and detection of fullerenes

Spectroscopic analysis provides reliable information on the nature of the process of formation of fullerenes and detection of the products. It is also a method by which fullerenes can be identified. For example, the meagre infrared absorption spectrum of the $C_{60}$ molecules is a direct indication of the high symmetry of these molecules and, in the final analysis, it provides an incontrovertible proof of their structure [6, 54, 108]. The infrared absorption spectrum of $C_{60}$ has four strong absorption lines centred at energies corresponding to 1429, 1183, 577, and 528 cm$^{-1}$; the widths of these lines vary in the range 3 – 10 cm$^{-1}$. If fullerene molecules are present in a gas in small amounts, their presence can be detected on the basis of these absorption lines. This has played a decisive role in the development of modern technology for the production of fullerenes, because a two-hump structure has been observed in the absorption spectrum of dust and attempts have been made to enhance this structure. If $C_{60}$ consists of the $^{13}C$ isotope, the absorption lines are shifted in the red direction. The energies of these transitions in the infrared absorption spectrum of $C_{60}$ agree approximately with the results of calculations [23, 109 – 113] carried out on the assumption that the $C_{60}$ structure represents a truncated icosahedron.

In view of its high symmetry, the $C_{60}$ molecule has a meagre absorption spectrum, but a rich Raman scattering spectrum. A detailed investigation of the Raman spectra of the $C_{60}$ and $C_{70}$ molecules, carried out with a spectral resolution of 9 cm$^{-1}$, was reported in Ref. [51]. Typical Raman scattering spectra of carbon dust deposited on a tungsten foil were obtained [51]. Lines with the frequencies 1568, 1232, 1185, 1062, and 260 cm$^{-1}$ were attributed to the $C_{70}$ molecule, whereas the lines at 1469, 497, and 172 cm$^{-1}$ were attributed to $C_{60}$. This was established by altering the $C_{70}$ content of the investigated sample.

It follows that Raman spectroscopy is a convenient method for the analysis of fullerenes. Table 2 lists the

**Table 2.** Raman frequencies, relative intensities, and depolarisation coefficients of Raman scattering lines of carbon soot containing fullerenes [51]. Values of $I_\perp$ and $I_\parallel$ represent different conditions during soot preparation.

| $\mu$/cm$^{-1}$ | $I_\perp$ | $I_\parallel$ | $\rho(\pm 0.02)$ | Identification |
|---|---|---|---|---|
| 260 | 7 | 34 | | $C_{70}$ |
| 273 | 17 | 17 | | $C_{60}, H_g$ |
| 413 | | 9 | | |
| 435 | 5 | 6 | | |
| 457 | | 9 | | |
| 497 | 27 | 27 | 0.16 | $C_{60}, A_g$ |
| 571 | 2 | 9 | | |
| 705 | | 13 | | |
| 711 | 4 | | | |
| 739 | | 13 | | |
| 773 | 6 | 13 | | |
| 1062 | 2 | 14 | 0.23 | $C_{70}$ |
| 1185 | 4 | 34 | 0.19 | $C_{70}$ |
| 1232 | 4 | 36 | 0.19 | $C_{70}$ |
| 1336 | | 11 | | |
| 1370 | | 11 | | |
| 1430 | 13 | | | |
| 1448 | | 32 | | |
| 1469 | 100 | 100 | 0.11 | $C_{60}, A_g$ |
| 1513 | 3 | 15 | | |
| 1568 | 15 | 88 | 0.24 | $C_{70}$ |

frequencies, relative intensities, and identifications of the Raman scattering lines of soot. In the case of the strongest lines the degree of depolarisation $\rho = I_{\perp}/I_{\parallel}$ of the scattered radiation is given; here, $I_{\perp}$ and $I_{\parallel}$ are the intensities of the scattered radiation with the polarisations perpendicular and parallel to the polarisation of the incident light. The high degree of polarisation of the scattered light representing the two strongest lines of $C_{60}$ (497 and 1469 $cm^{-1}$) demonstrates that these lines are due to totally symmetric vibrational modes of this molecule.

Let us consider separately the line with the frequency $\nu = 273$ $cm^{-1}$ on the basis of the experimental data given in Ref. [51]. This line has been the subject of many calculations carried out before this experimental study According to the calculations, the transition responsible for the line corresponds, on the basis of the truncated icosahedron model of the $C_{60}$ model, to the transformation of a sphere into an ellipsoid of revolution (gourd-shaped $P_n$ mode) and its frequency is $273 \pm 10$ $cm^{-1}$ [17–19, 30, 31]; the frequency scatter represents the result of statistical averaging of the results obtained by different authors. This is evidence in support of the truncated icosahedron model of the $C_{60}$ molecule. The 1469 $cm^{-1}$ transition corresponds, according to calculations, to elongation and compression of the pentagonal faces of the icosahedron and the 467 $cm^{-1}$ transition is due to 'breathing' vibrations. The calculated values of the frequencies of these transitions are not in very good agreement and they amount to 1627–1830 and 510–660 $cm^{-1}$, respectively.

The fullest information on the vibrational spectra of the $C_{60}$ molecule is provided by the spectra of inelastic scattering of slow neutrons by this molecule, because such scattering can excite efficiently all the vibrational modes of the molecule, irrespective of their symmetry [114–116]. According to an analysis given in Ref. [117], out of 174 possible vibrational modes of the $C_{60}$ molecule, we can identify 46 fundamental modes and among these two have the $A_g$ symmetry, one has $A_u$, three have $T_{1g}$, four have $T_{1u}$, five have $T_{2u}$, six have $G_g$, six have $G_u$, eight have $H_g$, and seven have $H_u$. All four vibrations with the $T_{1u}$ symmetry are active in the optical absorption spectra, ten vibrations with the $H_g$ and $A_g$ symmetry are active in the Raman scattering spectra, and the other vibrations do not appear in the optical spectra. Table 3 lists the frequencies corresponding to resonances in the energy loss spectra of neutrons scattered by the $C_{60}$ molecules at 20 K [115]. These values [115, 116], identified in accordance with the symmetry of the molecular vibrations, are compared with the data deduced from infrared absorption and Raman scattering spectra. It can be seen from this table that the fullest information on the vibrational spectrum of the investigated molecule is provided by inelastic neutron scattering. The unidentified neutron energy-loss peaks are evidently associated with the excitation of combination tones and overtones.

Production of higher fullerenes in macroscopic quantities [99] has made it possible to analyse the spectral characteristics of the molecules of these fullerenes, although not in as detailed a manner as in the case of $C_{60}$. The infrared absorption spectra of these molecules are more complex (see, for example, Refs [8, 82, 99, 118, 119]). In particular, the absorption bands of the $C_{76}$ molecule are located at the wavelengths 230, 286, 328, 350, 378, 405, 455, 528, 564, 574, 642, 709 and 768 nm [8, 99]. The absorption spectrum of the $C_{84}$ molecule contains bands at 280, 320, 380, 393, 476, 566, 616, 668, 760 and 912 nm. The results of a detailed investigation of the Raman scattering spectra of the $C_{76}$ molecule are given and analysed in Refs [82, 119].

**Table 3.** Comparison of the frequencies of vibrations of the $C_{60}$ molecule, determine by the inelastic neutron scattering, optical absorption, and Raman scattering methods [115].

| Identification | Frequency/$cm^{-1}$ | | |
|---|---|---|---|
| | neutron scattering | optical scattering | Raman scattering |
| Lattice vibrations | 96. 6 | — | — |
| Lattice vibrations | 145 | — | — |
| — | 234 | — | — |
| $H_g$ | 266 | — | 273 |
| $T_{2u}$, $G_u$ | 346, 354 | — | — |
| $H_u$ | 403 | — | — |
| $H_g$ | 443 | — | 437 |
| $G_g$, $A_g$ | 483 | — | 496 |
| $T_{1u}$ | 531 | 523 | — |
| $T_{1u}$ | 572 | 572 | — |
| — | 620 | — | — |
| — | 669 | — | — |
| $H_g$ | 708 | — | 710 |
| — | 740 | — | — |
| $H_g$ | 773 | — | 774 |
| | 837 | — | — |
| | 877 | — | — |
| | 919 | — | — |
| | 960 | — | — |
| | 1000 | — | — |
| | 1060 | — | — |
| $H_g$ | 1100 | — | 1100 |
| — | 1120 | — | — |
| $T_{1u}$ | 1180 | 1180 | — |
| — | 1200 | — | — |
| $H_g$ | 1260 | — | 1250 |
| — | 1350 | — | — |
| $H_g$, $T_{1u}$ | 1420 | 1430 | 1430 |
| $A_g$ | 1480 | — | 1470 |
| $H_g$ | 1580 | — | 1570 |

## 4. Nanotubes and endohedrals

### 4.1 Structure of nanotubes

The process of formation of fullerenes from graphite yields also various structures which are composed, like graphite, of six-member carbon rings. These structures are closed and empty inside. They include nanoparticles [4, 120] and nanotubes [4, 5]. The nanoparticles are closed structures similar to fullerenes, but of much larger size. In contrast to fullerenes, they may contain several layers. Such multilayer spherical structures are called onions. The nanotubes are elongated structures consisting mainly of six-member carbon rings.

Fig. 8 shows the structure of nanotubes formed by an arc discharge at a temperature of the order of 3000 K in the region where fragments of the investigated structures are formed. Electron microscopy makes it possible to distin-

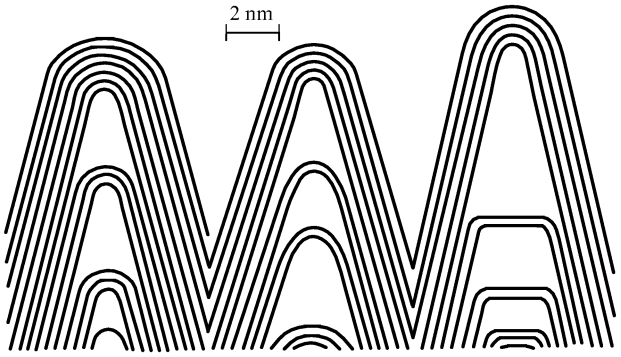


**Figure 8.** Sections of the free ends of microtubes, recorded with an electron microscope [5]. Each line represents a separate layer consisting of hexagons (in the rectilinear part) or of combinations of hexagons and pentagons (in the rounded part). The distance between the adjacent layers is 0.34 nm.

guish the various layers of a structure separated, as in graphite, by 0.34 nm. The schematic diagram in Fig. 8 shows the most common nanotubes. They are extended multilayer structures with rounded ends. One end is attached to a surface and the other is free. Under certain conditions one can also observe the formation of single-layer nanotubes with the diameter ranging from 1 to 6 nm [33, 121]. It is obvious that the effective formation of nanotubes is possible in the presence of extended graphite fragments, which are very different from the fragments shown in Fig. 3 used as the starting material in the preparation of fullerenes. One of the ways of forming such extended graphite fragments is discussed in Ref. [123]. Excitation of graphite may produce $sp^3$ defects in the $sp^2$ networks forming the graphite planes. The appearance of these defects, directed along the graphite network lines, has been observed with the aid of an atomic microscope and a scanning tunnelling microscope [123] as a result of bending and breaking of the graphite planes. It is possible that breaking of the graphite planes along such defect lines can produce extended fragments.

The subsequent transformation of these extended fragments, which are products of thermal decomposition of graphite, into closed structures (nanotubes) should occur only under special conditions. We must bear in mind that, in addition to these extended graphite fragments, there are many more small fragments which then join together to form fullerenes. The interaction of the small fragments with the extended ones interferes with the formation of nanotubes. Experience has shown that the optimal conditions for the formation of nanotubes are obtained in an arc discharge. The high radial temperature gradients in such a discharge evidently provide the optimal relative positions of the regions where extended graphite fragments twist to form tubes and are quenched in this state. This rough outline shows that the probability of formation of nanotubes from graphite is low, i.e. that the relative content of nanotubes in the products of transformation of graphite is small. Under optimal synthesis conditions this content does not exceed a few percent.

The characteristic features of the nanotube structure include components of the graphite and fullerene structures. Separate graphite fragments, representing a certain set of hexagons, form the base of a nanotube. Joining of such hexagonal fragments into a three-dimensional closed structure requires the presence of a certain number of pentagons, which are responsible for the rotation of the hexagonal network in space and transformation of this network from a planar to a three-dimensional structure. Carbon nanotubes reflect the variety of the forms of carbon which are formed under high-temperature nonequilibrium conditions.

Since nanotubes are the result of twisting of extended graphite fragments, many features of the graphite structure should be retained also in nanotubes. In particular, in the case of a multilayer nanotube the distance between its layers should be close to the distance between the graphite planes, which amounts to 0.3354 nm. Measurements [124] indicate that the average distance between the adjacent layers in a nanotube with a diameter of 7 nm is $0.344 \pm 0.001$ nm. Obviously, the change in the average distance between the nanotube layers depends on the tube radius, the number of layers, and the environment. If a nanotube lies on a substrate, the distance between the adjacent layers depends on the nature of this substrate. Moreover, the interaction with the substrate distorts the cylindrical shape of a nanotube. This applies also to the interaction between two nanotubes [125].

A nanotube can be formed as a result of twisting of an extended graphite fragment in such a way that its extended edges join. Joining of the sides of a fragment can be achieved in a variety of ways. In the simplest case a nanotube has the cylindrical symmetry, so that the line passing along the sides of the hexagons in a fragment and perpendicular to the line of break in the network may be inscribed into a circle after the fragment is twisted into a tubule. However, other ways of joining extended sides of a fragment are possible and these differ from that just indicated by the relative displacement of the sides to be joined by a finite number of hexagons. A nanotube formed in this way has the chiral symmetry.

Twisting of an extended graphite fragment into a nanotube creates stresses in the hexagonal components of the structure. This affects the properties of a nanotube, which may depend on the nanotube diameter and on its chirality. In particular, the conduction in a nanotube may be semiconducting or metallic, depending on its diameter and chirality [122, 126–129]. It is obvious that the smaller the nanotube diameter, the greater the stress resulting from its formation. Nevertheless, nanotubes with a diameter varying in a wide range of values, right down to the diameter of the $C_{60}$ fullerene molecule, have been observed [130].

### 4.2 Production and properties of nanotubes

A nanotube may be formed from extended graphite fragments, which are then twisted into a tube as described above. Special conditions during heating of graphite are necessary for the formation of extended fragments. Experience shows that the optimal conditions for the formation of nanotubes are realised in an arc discharge when electrolytic graphite is used as the electrode material. An arc discharge takes place in an inert gas at a pressure of about 1 bar and the voltage between the electrodes is tens of volts when the distance between them is of the order of 1 cm. A discharge current of the order of 100 A ensures heating of the gas in the positive discharge column to a temperature of about 3000 K. This discharge current evaporates the anode. Other products of the thermal evaporation of the graphite anode include nanotubes

attached partly to the cold surfaces of the apparatus and partly deposited on the surface together with soot. This general procedure for the formation of nanotubes has been used in all the experiments beginning from those reported in Refs [4, 5].

The processes described above produce mainly multilayer nanotubes and among the products obtained under optimal conditions the nanotubes represent only a small fraction: their yield does not exceed a few percent. The other products are fullerenes, nanoparticles, and other soot particles. The most effective, in respect of the formation of nanotubes, are the subsequent processes which make it possible to increase the proportion of nanotubes in a mixture, 'undress' them by converting multilayer into single-layer structures, and open up their ends. Filling of open nanotubes with another material, producing fundamentally new objects, is highly promising. We shall now consider briefly these methods.

One of the problems experienced in the formation of nanotubes is to ensure that they consist of a single layer. It has been found that this can be done by including transition metals in the anode material. Single-layer nanotubes are produced when the anode contains a small amount of Fe [32], Co [33], Ni [131], and Gd [132]. Another method for the production of single-layer nanotubes is oxidation. This method is interesting because it makes it possible to separate the anode tubes from other components of soot. The first stage is some standard method of the same kind as used in the separation of fullerenes: filtering of soot solutions, centrifuging, and chromatogaphic separation. All these methods make it possible to separate nanotubes from fullerenes, but not these tubes from nanoparticles. Oxidation of the deposited soot provides a better opportunity for separating nanotubes from nanoparticles and, moreover, the upper layers can be removed from a multilayer tube and its ends can be opened [36].

The oxidation method is based on the difference between the reactivities of nanotubes and nanoparticles. The reactivity of nanoparticles is higher and, therefore, when the degree of decomposition of the carbon product by oxidation is high, the proportion of nanotubes in the residue increases. Measurements reported in Ref. [36] indicate that nanoparticles are destroyed almost completely by 99% oxidation of the product and after 95% oxidation the content of single layer nanotubes in the remaining material is 10% – 20%. Nanotubes are oxidised either by treatment with oxygen in the course of moderate heating [36] or by immersion in boiling nitric acid [133]. The latter treatment removes five-member graphite rings and opens up the tube ends.

The oxidation process can not only remove other components of the product and the outer layers of a nanotube, but it can also open up its ends. Obviously, this can be achieved also by other chemical reactions employing the different rates of participation in these reactions of the carbon located at different places on a nanotube. For example, one can use the reaction of carbon with hot carbon dioxide [35], as a result of which carbon is transformed into gaseous carbon monoxide taking away one oxygen atom from the dioxide molecule. It is found that the carbon atoms in pentagonal rings are chemically more active. These carbon atoms react chemically with carbon dioxide and form a gaseous phase. Since these pentagonal rings are at the ends of the nanotube, the process results in the opening of its ends.

A nanotube with open ends is a physical object with novel and interesting properties. It can be used as a capillary, sucking in atoms whose dimensions are comparable with the inner diameter of the tubule. This effect, predicted theoretically in Ref. [134], had been detected experimentally [34]. It was found that molten lead was pulled into some nanotubes and filled them internally. This method was used to form a nanowire with a shell of diameter less than 1.5 nm. The properties of a metal in such a tube differ, because of the small internal diameter, from the properties of bulk metal and the interaction with carbon results in a further change in the properties of the metal.

An even more striking example, illustrating the very promising applications of nanotubes in materials science, is provided by a recent paper [183] reporting the formation of superconducting TaC crystals inside carbon nanotubes. A dc ($\sim$30 A) arc discharge operating at a voltage of 30 V in a helium atmosphere (at a pressure of 100 – 300 Torr) was used. The electrodes represented a compacted mixture of a thallium powder with a graphite cement in the weight ratio 0.6. The gap was 2 – 3 mm. Tunnelling electron microscopy revealed that the thermal decomposition of the electrode material produced a considerable number of TaC crystals which were encapsulated inside the nanotubes. A typical transverse dimension of these crystals was about 7 nm and a typical nanotube length was in excess of 200 nm. These tubes were multilayer cylinders with a distance $3.481 \pm 0.009$ A between the layers, which was close to the corresponding value for graphite. The temperature dependence of the magnetic susceptibility of the resultant samples showed that such an encapsulated nanocrystal, like macroscopic TaC crystals, became superconducting at $T = 10$ K. This way of making superconducting crystals encapsulated in nanotubes means that these crystals can be isolated from the undesirable effects of the ambient medium (in particular oxidation in this medium), promising a way for a more effective development of the appropriate nanotechnologies.

The development of such technologies should yield new physical objects with properties of scientific and practical interest.

### 4.3 Endohedrals

As early as 1985, Kroto et al. [3], who were the first to suggest that the structure of the $C_{60}$ clusters represents regular truncated icosahedra, discussed the possibility of intercalation of such clusters with atoms of different kinds. Soon after the publication of this paper, the first reports appeared of the observation of compounds of this type, as evidenced by the mass spectra of the products of laser thermal evaporation of graphite, the structure of which included a lanthanum-intercalated powder. It was found that at a sufficiently high laser radiation intensity ($1 - 2$ mJ cm$^{-2}$) the mass spectrum contains peaks, which have been attributed to the compound $LaC_{60}$ where a lanthanum atom is inside a fullerene cage. These compounds have since been called the endohedral compounds or complexes and they are denoted by the symbol $M@C_{2n}$ [139], in contrast to ordinary chemical compounds of the $MC_{2n}$ type in which the attached M atom is located outside a fullerene cage. The existence of endohedrals has been questioned for a long time [136, 137], primarily because of their low concentration in fullerene-carrying

soot and the difficulties encountered in their experimental identification. Many experimental papers have now been published on the formation of endohedral complexes and on their properties. An analysis of these papers leaves no doubt about the existence of such compounds. The list of elements whose atoms can be intercalated into a fullerene cage is growing continuously and at present amounts to about one-third of the periodic table [37]. A detailed review of the current status of the topic of endohedrals can be found in Ref. [138]. A brief discussion of this topic will now be given and some of the data will be taken from Ref. [138].

The most effective technology for the production of endohedral complexes is based on the same approach as the technology for the production of fullerenes described above. Soot, containing not only fullerenes but also endohedral complexes, may be formed by thermal evaporation of graphite which is mixed with a powder of a metal or its oxide to be intercalated in a fullerene [139, 140]. Under the optimal conditions the yield of endohedrals does not exceed a few percent of the fullerene yield. A further increase in the efficiency of synthesis of endohedrals and widening of the list of the compounds which can be produced in this way have been achieved by the use of graphite electrodes in the form of hollow cylindrical tubes, filled with a mixture of metal (or a metal oxide) powder and a graphite dust [141–143], or a plasma jet with electrodes made of a mixture of activated carbon and a metal oxide [144], or an arc with graphite electrodes burning in an $He + Fe(CO)_5$ atmosphere [145, 146]. Good yields of endohedrals are also possible if metal carbides are used as the starting materials [147]. In all these methods for the preparation of soot containing fullerene with an admixture of endohedrals it has been found that, although the relative fraction of endohedrals in soot increases with increase in the relative content of a metal in the starting material, this fraction never exceeds a few percent. An increase in the endohedral fraction in the products of thermal decomposition of graphite is usually accompanied by a fall of the overall yield of fullerenes in soot [148].

Under conditions favourable for the formation of endohedrals it is usual to find a wide range of endohedral molecules. The products of thermal decomposition of graphite mixed with scandium [30] include endohedrals differing from one another not only in respect of the size of the fullerene cage, but also in the number of intercalated scandium atoms. The mass spectrum is dominated by $Sc_2@C_{82,84,86}$ endohedrals containing two scandium atoms each. Among the endohedrals containing one and three scandium atoms predominate compounds such as $Sc@C_{82}$ and $Sc_3@C_{82}$.

The full list of various types of endohedrals, detected in the mass spectra of soot containing fullerenes, is very long and is continuously being added to. For example, in addition to the molecules mentioned above, this list includes a whole group of molecules such as $Y@C_{2n}$, $30 < n < 50$, $Y_2@C_{82}$ [149], $U@C_{28}$, $U@C_{60}$ [150], $He@C_{60}$ and $Ne@C_{60}$ [151], $CO@C_{60}$ [152], $CN@C_{60}$ [153], $Ca@C_{60}$, $Sr@C_{60}$, $Sm@C_{60}$, $Eu@C_{60}$ and $Yb@C_{60}$ [154], $Gd@C_{82}$ and $Gd_2@C_{82}$ [155], $Pr@C_{82}$ and $Lu@C_{82}$ [156], etc. However, it should be stressed that the presence of a particular type of an endohedral complex in the mass spectrum of soot containing fullerenes does not necessarily mean that such a complex can exist in a stable form and be separated as a complex. For example, endohedral complexes are formed by the $C_{60}$ fullerene with the atoms of Ca, Sr, Sm, Eu, and Yb and can be seen quite clearly in the relevant mass spectra, but attempts to separate these compounds by the method of sublimation and subsequent thermal desorption have resulted in their decomposition [154]. We can assume that the stability of endohedral complexes increases with the size of the relevant fullerene shell.

Endohedrals are separated and purified by the same approaches as those used in the separation and purification of fullerenes. This approach, based on the different sorption activities of different endohedrals in solutions in relation to specific sorbents, represents varieties of liquid chromatography. In the realisation of this approach it is essential above all that an endohedral to be isolated should have a sufficient solubility in those solvents which can be used in liquid chromatographs. Recent investigations [138, 142, 143, 157–165] show that the solubility of $Sc@C_{82}$, $Y@C_{82}$, $La@C_{82}$, $La_2@C_{80}$, $La_2@C_{82}$, $Y_2@C_{80}$, $Y_2@C_{82}$ endohedral complexes in toluene, pyridine, and $CS_2$ are of the same order of magnitude as the solubility of higher fullerenes in these solvents. This makes it possible to separate such endohedrals in their pure form and to investigate the physicochemical properties of both single molecules and of condensed bodies made of them.

The technology of separation and purification of endohedral complexes, based on high-pressure liquid chromatography, is characterised by an extremely low productivity. The most efficient equipment is capable of producing pure endohedral complexes at a rate of tens of microgrammes per hour. This is the reason why the investigations of endohedral compounds, started practically at the same time as the studies of fullerenes, are still in the early stages. The main result of these investigations is the experimental proof of the structure of these compounds. Let us consider this proof in greater detail. One of the ways of proving that an atom of a given kind is inside a fullerene structure involves an investigation of the thermal decomposition channels of the relevant compounds [166]. Experiments have shown [166] that thermal decomposition of $LaC_{82}$ is accompanied by splitting off of $C_2$ and not La fragments, as one would expect in the case of a lanthanum atom located on the outer side of a fullerene cage. The same molecule behaves similarly in thermally initiated chemical reactions. One further experimental confirmation of the characteristic structure of endohedral compounds was provided by a study of the collisions of the $LaC_{82}$ molecule with a solid surface [167]. The experimental results demonstrated that collisions with energies less than or of the order of 200 eV do not result in the loss of a metal atom. It is difficult to see how such a molecular stability, typical of fullerenes, would have been possible with a metal atom outside the fullerene cage. Similar results follow from studies of collisions between endohedral fullerene complexes and rare-gas atoms [168–177]. In a review of the experimental results confirming the endohedral structure of some metal–fullerene complexes, it is worth considering the report of two modifications of the compound of yttrium with $C_{60}$ [178]. A comparision of the reactivities of these modifications, relative to the reaction with $N_2O$, revealed that the $YC_{60}$ molecule belonging to the first modification readily reacts with $N_2O$ forming as the final product the compound YO, but molecules of the second modification hardly react. This is evidence that the molecules of the second modification have the endohedral structure.

However, the most convincing proof of the endohedral structure of metal–fullerene complexes has been provided by modern physical analysis methods, such as ESR, photoelectron, Mossbauer, and x-ray absorption spectroscopy. ESR spectroscopy makes it possible to obtain detailed information on the electron structure and the chemical state of atoms in some metal–fullerene compounds, demonstrating their endohedral structure. For example, the ESR spectrum of the $LaC_{82}$ molecules [140] has eight equidistant hyperfine splitting lines of the $^{139}La$ nucleus, indicating that the ionic structure of this compound is of the $La^{3+}C_{82}^{3-}$ type. An analysis of the electronic structure of the $C_{82}^{3-}$ negative ion shows that such a structure is possible only for an endohedral position of the lanthanum atom in the fullerene cage. Measurements of the x-ray absorption band edges make it possible to determine the chemical state of the atoms in a compound. Application of this method to the $YC_{82}$ metal–fullerene compound showed [179] that the yttrium atom is outside the fullerene lattice. However, this was in conflict with the experimental results reported in Ref. [149] where x-ray photoelectron spectroscopy was used to conclude that the fullerenes $LaC_{2n}$, $YC_{2n}$, and $Y_2C_{2n}$ have the endohedral structure. This conclusion follows the measurements that indicate the +3 valence of the metal atom in this compound. A similar conclusion was reached in Ref. [150] on the basis of the x-ray photoelectron energy spectrum of the compound $UC_{28}$ indicating that the valence of the uranium atom is +4 and, therefore, it is located inside the fullerene lattice. The same situation occurs in the case of $CaC_{60}$, as concluded from an investigation and analysis of the photoelectron spectra reported in Ref. [180].

Further progress in the investigation of endohedrals and of the possibility of using these compounds in scientific and practical applications will be determined primarily by the development of a technology for the synthesis and strong purification of these materials. These compounds are expected to be superconducting [14, 15]. The chemical inertness of the metal atoms intercalated in endohedral fullerenes, pointed out by R E Smalley, opens up new opportunities for the storage of toxic and radioactive materials. The possibility of constructing solid-state lasers from endohedral compounds has been discussed [138]. Intercalation of refractive metal atoms, such as uranium, in the fullerene lattice may prove to be one of the effective methods for the preparation of soluble or volatile compounds of such metals without recourse to fluorination [30]. Endohedral fullerenes, containing polar molecules, may provide the basis for new ferroelectric materials [181, 182].

## 5. Fullerenes in gaseous systems

### 5.1 Thermodynamics of fullerenes and processes involving them

Before we consider the thermodynamic characteristics of fullerenes in the gaseous state, we shall list some of the parameters of the $C_{60}$ molecule. This molecule is electronegative, its electron affinity is 2.65 eV [184], and its ionisation potential is 7.61 eV [185]. The binding energy, calculated per one carbon atom in this molecule, is 7 eV [186] and the polarisability calculated in Ref. [187] is close to 80 $A^3$.

Under normal conditions, fullerenes are in the condensed state and usually crystalline. At room temperature the saturated vapour pressure of fullerenes is negligible, but it is significant at temperatures above 600 K. It follows from the results of measurements reported in Ref. [188] that in the temperature range 600–800 K the saturated vapour pressure varies with temperature in accordance with the Arrhenius law:

$$\log_{10}\left(\frac{p}{p_a}\right) = -\frac{A}{T} + B\,,$$

where $B = 11.582 \pm 0.126$ and $A = 9777 \pm 138$ K. We can see that at these temperatures the saturated vapour pressure ranges approximately from $10^{-5}$ to 0.2 Pa. The sublimation energy of $C_{60}$ at $T = 700$ K is $43.3 \pm 0.5$ kcal mol$^{-1}$ or 1.9 eV. This is supported by the results of Ref. [189], which showed that the heat of sublimation of $C_{60}$ exceeds 39 kcal mol$^{-1}$. The heavier fullerene $C_{70}$ is even less volatile: the saturated vapour pressure above this fullerene in its pure state is about 0.1 Pa at $T = 800$ K and the parameters in the Arrhenius temperature dependence are $A = 10219 \pm 78$ K [188] and $9848 \pm 229$ K [213]; $B = 11.596 \pm 0.065$ [188] and $11.224 \pm 0.071$ [213]. The lower volatility of $C_{70}$, compared with $C_{60}$, is not only due to the higher mass of the former molecule, but also and mainly due to the higher heat of sublimation, which amounts to about 46 kcal mol$^{-1}$ at $T = 760$ K [188]. The partial saturation vapour pressures of $C_{60}$ and $C_{70}$ above a solid solution differ considerably from the corresponding values above a crystalline fullerite with the same partial composition [188].

The strong temperature dependence of the saturated vapour pressure of fullerenes is used in the technology for thorough purification of these materials, which is intended to remove volatile impurities and fullerene molecules of other types [190, 191]. It should be pointed out that, like diamond, the fullerene molecules represent a metastable modification of carbon. The energy needed for the formation of the $C_{60}$ molecule from graphite is calculated to be 0.4 eV per one carbon atom, whereas in the case of diamond the same parameter is 0.02 eV [67]. The energy barrier that has to be overcome in such a change in the carbon structure is considerably higher than the values given above.

The high binding energy of the carbon atoms in fullerene molecules and the symmetry properties of these molecules are responsible for their anomalously high thermal stability. The results of a numerical simulation, based on the molecular dynamics method [192, 193], demonstrate that the $C_{60}$ molecules lose their chemical structure only as a result of heating to temperatures above 3000 K.

The results of investigations of the processes involving $C_{60}$ and other fullerenes are also evidence of an anomalously high stability of these carbon compounds. The same conclusion follows from the very first experiments which revealed that $C_{60}$ behaves as a cluster with a magic number of atoms. An investigation of monomolecular dissociation of carbon clusters with $n \geqslant 30$ has shown that the stability of clusters with even values of $n$ is considerably higher than the corresponding stability of clusters with odd $n$. Both in monomolecular dissociation [49] and in photodissociation [194], the main channel for the dissociation of $C_n$ molecules with even values of $n$ involves splitting off a $C_2$ fragment. This is surprising, since the binding energy of a $C_2$ fragment is less than the corresponding value for $C_3$ [195]. In dissociation of $C_n$ clusters with odd $n$, the

most likely process is the splitting off of a carbon atom. We thus have a situation in which clusters with even values of $n$ can survive and the fraction of clusters with odd $n$ does not exceed 1% [194]. These experimental observations provide information on the structural characteristics of $C_n$ clusters with a large value of $n$, such as the absence of sharp angles and faces [49, 196–198].

An investigation of the nature of the dissociation of fullerenes under the action of ultraviolet radiation throws additional light on the nature of the stability of these compounds. A recent series of papers [199, 200] is worth noting: they report the mass spectra of the neutral products of dissociation of the $C_{60}$ cluster subjected simultaneously to the action of photons with $\lambda = 308$ nm and 118 nm. A fairly complex apparatus was used in this investigation and it included in particular three sources of laser radiation emitting at different wavelengths. The second harmonic from a Q-switched laser ($\lambda = 532$ nm) was used to evaporate $C_{60}$ molecules deposited on a stainless steel substrate. The photodissociation of $C_{60}$ in the gaseous phase resulted from exposure to XeCl laser radiation with $\lambda = 308$ nm. Neutral fragments produced by the photodissociation of $C_{60}$ were ionised by radiation with $\lambda = 118$ nm, which was generated by double tripling of the neodymium laser frequency. An analysis of time-of-flight mass spectra of the neutral products of the photodissociation of $C_{60}$ indicated that the dissociation involved the absorption of a certain number ($\sim 10$) of $\lambda = 308$ nm laser photons by a molecule. The energy of the electronic excitation as a result of absorption of a laser photon by a molecule is rapidly converted into the energy of molecular vibrations, which becomes distributed in a statistical manner between a large number of the degrees of freedom of the molecule. Recent calculations [201] demonstrated that the $C_{60}$ molecule, with the minimum dissociation energy $\sim 4.6$ eV, can dissociate in the time of flight in a mass spectrometer ($\sim 10^{-5}$ s) and its internal energy should exceed 30 eV. This agrees with the results of the experiment discussed above in which, in addition to $C_2$, the recorded dissociation products included larger carbon clusters with an even number of atoms.

A higher stability of fullerenes with a closed symmetric structure is indicated also by the results of experiments on pair collisions involving these molecules. For example, it was established [202] that out of a large number of the $C_n^{z+}$ carbon clusters with $n = 60-124$ and with $z = 2$ or 3, only the $C_{60}^{z+}$, $C_{70}^{z+}$, and $C_{84}^{z+}$ clusters retain their structure after charge exchange with the $C_7H_8$ molecule. The collisions of these cluster ions with Xe atoms at 392 eV produce $C_{60}^{2+}$ ions, and collisional dissociation of these ions requires an energy greater than or of the order of 1 keV [49, 194, 197, 203].

Dissociation of the $C_{60}^{+}$ cluster in collisions with the $O_2$ molecule of 7–8 keV energy had been investigated earlier [204]. Collisions produced not only smaller clusters, but also multiply charged $C_{60}^{z+}$ clusters, where $z = 2-4$. This is evidence of the possibility of collisional ionisation of the $C_{60}^{+}$ cluster without its fragmentation. This is additional evidence for the exceptionally high stability of fullerenes.

The ion–molecule reaction of the $C_{60}$ cluster with $C^+$ in the collisional energy range 2–78 eV has also been investigated [205] and the reaction channels were identified by the nature of the $^{13}C^+$ isotope. It follows from these measurements that at collision energies in excess of 10 eV the main reaction channel is the formation of a long-lived $C_{61}^{+}$ complex, which dissociates after a time exceeding $10^{-3}$ s. Further dissociation of this complex may be accompanied by charge transfer, i.e. by the escape of a neutral carbon atom. The most probable is the charge transfer process accompanied by isotopic exchange, as a result of which the fragment is a carbon atom which is initially in the $C_{60}$ structure.

Interesting features of the behaviour of fullerenes had been discovered in a study of collisions of these molecules with the surface of a solid [206–209]. For example, it was established [206] that collisions of charged $C_{60}^{\pm}$, $C_{70}^{\pm}$, and $C_{84}^{\pm}$ fullerenes with the surface of purified graphite and silicon, at energies ranging from zero to 200 eV, result in the loss of a considerable part of the kinetic energy but are not accompanied by the dissociation of fullerenes. Similar conclusions were also reached in Ref. [209] reporting an investigation in which the collisional energy of charged $C_{60}^{+}$ clusters with the surface of purified graphite ranged from 150 to 450 eV. It was established that the ion scattering angle corresponded to near-specular reflection from a surface, whereas the kinetic energy of the scattered ions was 10–20 eV, irrespective of the collisional energy.

### 5.2 Chemistry of fullerenes

The structure of fullerenes makes it possible to consider them as three-dimensional analogues of aromatic compounds. Consequently, the chemistry of fullerenes can be regarded as one of the most promising directions in organic chemistry. The main concepts in the chemistry of fullerenes and the most important practical progress made in the synthesis of new fullerene compounds are described in detail in recent reviews [210–212]. More detailed information can be found in these reviews, whereas here we shall recount briefly the main trends in the development of the chemistry of fullerenes and the main problems facing investigators.

As pointed out earlier, fullerenes are distinguished by a high chemical inertness in respect of the process of monomolecular dissociation. For example, measurements reported in Ref. [214] indicate that the $C_{60}$ molecule remains thermally stable at temperatures up to 1700 K and the monomolecular dissociation rate constant varies within the range 10–300 $s^{-1}$ at temperatures 1720–1970 K. This dissociation rate corresponds to a dissociation activation energy of $4.0 \pm 0.3$ eV. However, in the presence of oxygen (particularly in open air), oxidation of this form of carbon is accompanied by the formation of CO and $CO_2$, and is observed at much lower temperatures. It follows from the results of calorimetric measurements [189, 215] that intensive oxidation of $C_{60}$ is observed even at temperatures of the order of 500 K. The process lasts several hours and it produces an amorphous structure in which there are twelve oxygen atoms per each original $C_{60}$ molecule. The $C_{60}$ molecule loses almost completely its initial shape. A further increase in temperature to 700 K is accompanied by a rapid formation of CO and $CO_2$, and it results in final dissociation of the ordered fullerene structure. The total heat of oxidation of $C_{60}$, found by a calorimetric method, is approximately 53 kcal $mol^{-1}$ and the activation energy of the oxidation process is 58.2 kcal $mol^{-1}$ [189]. It follows from the experimental results that the energy for the attachment of an oxygen atom to the $C_{60}$ molecule is about 90 kcal $mol^{-1}$, which is approximately twice the corresponding value for graphite [216]. A comparison of these values makes it possible to find the energy required for the formation of the $C_{60}$ fullerene molecule from graphite with the same number of carbon atoms: $\Delta H = 540-600$ kcal -

$mol^{-1}$. This is of the same order of magnitude as the theoretical estimate $\Delta H \sim 800$ kcal $mol^{-1}$ [217].

The room-temperature oxidation of $C_{60}$ occurs only in the presence of illumination with photons of energies 2–1200 eV or 0.5–5 eV [218]. This is attributed to the need of formation of negative $O_2^-$ ions, which have a higher reactivity at room temperature [218].

Since the fullerene molecules have an electron affinity, they act as weak oxidants in chemical processes [210]. This property of fullerenes was discovered in one of the first experiments on their chemical transformations [99] in which the hydrogenation of $C_{60}$ was studied. The product of hydrogenation was the $C_{60}H_{36}$ molecule. This result is quite surprising because the structure of the $C_{60}$ molecule includes thirty double bonds, each of which could have participated in the attachment of two hydrogen atoms. In view of this, one would expect formation of the compound $C_{60}H_{60}$. Obviously, some of the double bonds in the $C_{60}$ structure are left without hydrogen atoms. According to a suggestion in Ref. [99], there are two single bonds between each such double-bond pair on the surface of a sphere.

It should be pointed out that the problem of fullerene hydrogenation is particularly important in the chemistry of fullerenes. This is because of the possibility of using fullerenes as the means for effective storage of molecular hydrogen [219] and in connection with the development of new battery cells based on fullerenes [37]. Fullerene hydrides have been synthesised by a variety of methods in many laboratories. Among publications on this topic one should mention particularly that in which the compound $C_{60}H_{36}$ with a small admixture of $C_{60}H_{18}$ was obtained as a result of the Birch reduction reaction. The same compound was reported in Ref. [221], where the same purpose was served by the reaction of transfer of a hydrogen atom between $C_{60}$ and a molecule of 9,10-dihydroanthracene. The compounds $C_{60}H_{36}$ and $C_{70}H_{36}$ were obtained also from fullerenes using iodoethane, heated to 673 K, as the source of atomic hydrogen [222]; the same compounds were produced also by treating cold fullerenes with hydrogen at a high pressure (about 70 bar). It follows from the experimental results [223] that under certain conditions the $C_{60}$ molecule can act like a sponge and absorb simultaneously and reversibly up to seventeen hydrogen atoms. The simplest fullerene hydride $C_{60}H_2$ was synthesised [224] by the reaction of $C_{60}$ with $CH_3$ in a solution where tetrahydrofuran was mixed with toluene. Obviously, the most direct fullerene hydrogenation method is the reaction in the solid phase at a high hydrogen pressure (up to 850 bar) at elevated temperatures (of the order of 600 K) [219] (see also Ref. [243]). The reaction products were found to be compounds of the $C_{60}H_y$ and $C_{70}H_x$ type, where $x = 2-18$ and $y = 4-30$.

One of the promising topics in the chemistry of fullerenes is the synthesis of water-soluble compounds of these molecules. The solution of this problem should make it possible to create a new class of biologically active substances for pharmaceutical purposes. An important step in this direction was made by the synthesis of a compound formed by a fullerene molecule with a large number (about 26) hydroxyl groups. This molecule is essentially a fullerene alcohol and it is shown in Fig. 9. Synthesis of this compound was carried out in an aqueous solution of NaOH using tetrabutylammonium hydroxide as a catalyst [368].

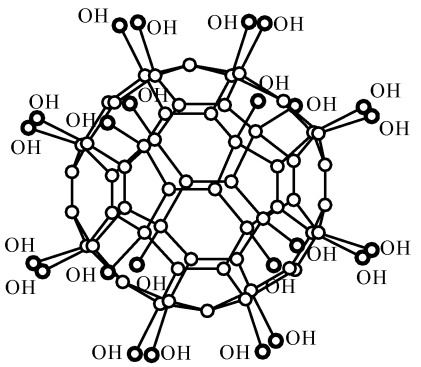


**Figure 9.** Chemical structure of a water-soluble fullerene, representing a $C_{60}$ molecule with attached OH radicals [368].

One other important topic in the chemistry of fullerenes, attracting considerable interest from specialists, is the synthesis of stable fluorine compounds of fullerenes. This interest is maintained to some degree by the hope to create solid lubricants, similar to Teflon, from fluorinated fullerenes. Such compounds are expected to have good lubricating characteristics even at very low temperatures. In spite of the considerable experimental and theoretical activities [190, 225–235], it is not yet clear whether this is possible. Soon after the publication of a report [225] of preparation of fully fluorinated fullerene $C_{60}F_{60}$, it was found that its chemical stability is very low [228, 229], because — in spite of the hydrophobic properties typical of fluorides — this compound readily reacts with water to form HF. This is accompanied by destruction of the fullerene structure of the molecules. Subsequent experiments [190, 226] on fluorination of fullerenes $C_{60}$ and $C_{70}$ yielded the compounds $C_{60}F_{36}$ and $C_{70}F_{44}$. Even these preliminary results [190, 226] indicated the suitability of these compounds as lubricating materials. A comparison of the results of many experimental investigations shows that the composition of the products of fluorination of fullerenes is largely determined by the conditions during the synthesis. For example, the reaction of $C_{60}$ with NaF at $T = 500-550$ K produces mainly $C_{60}F_{46}$ with a 10%–15% admixture of $C_{60}F_{48}$ [232, 233]. An increase in the fluorination temperature and duration results in the predominance of the $C_{60}F_{48}$ structure in the fluorination products [235] and this structure has apparently the highest stability.

Chlorination of $C_{60}$ produces a compound which contains either twelve [236] or twenty four [237] chlorine atoms. An attractive feature of chlorine compounds of fullerenes is the ability to replace the chlorine atoms with methoxy groups [237], which widens the class of fullerene compounds. This feature, although to a lesser degree, is found also in fluorinated fullerenes [228, 229]. Heating of the chlorine compounds of fullerenes is accompanied by regeneration of the $C_{60}$ molecule. The compound formed by the reaction of $C_{60}$ with bromine contains up to twenty eight bromine atoms [238, 239].

The very first experiments on the synthesis of organic compounds containing fullerenes provided evidence of a very great variety of these compounds. For example, twelve compounds of $C_{60}$, synthesised by Wudl's group, were described in Ref. [240]. Among such 'fulleroids' one could mention the products of the attachment of hydrogen and

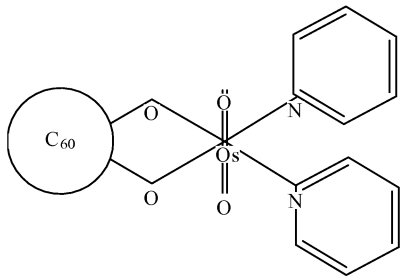


**Figure 10.** Structure of osmylated $C_{60}$ [242].

phosphorus radicals, of halogens, of metals and their oxides, of single and double benzene rings and their derivatives, of $NO_2$ [210], and of alkyl radicals [241]. Specialists were greatly interested in the results reported in [242] (for a review, see also Ref. [243]): the reaction of $C_{60}$ with $OsO_4$ produces metallo-organic compounds $C_{60}(OsO_4)$(4-tert-butyl-pyridine)$_2$, which is a ferromagnet. The structure of this compound, established in a series of elegant experiments, is shown in Fig. 10. Subsequent work by other authors confirmed [244] the hypothesis of extensive opportunities for the development of metallo-organic chemistry of fullerenes. There have been reports also of the preparation and investigation of such metallo-organic complexes as $[(C_6H_5)_3P]_2X(C_{60})$ [245], $[(C_6H_5)_3P]_2(CO)ClX(C_{60})$ [246], $\{[(C_2H_5)_3P]_2X\}_6C_{60}$ [245], where the symbol X denotes metals belonging to the platinum group: Pt, It, Pd. According to the results reported in Ref. [244], the attachment of a metal-carrying organic radical to a fullerene reduces the electron affinity of the fullerene. This alters the electric properties of the fullerene and opens up an opportunity for creating a new class of organic semiconductors with parameters varying over a wide range.

One other important direction in the development of the chemistry of fullerenes is related to the possibility of the synthesis of polymers on their basis [210]. The $C_{60}$ molecules can then play a dual role: they can act as the basis of a polymer chain, or perform the role of a connecting component. In the former case, when the result is described by the highly descriptive name of the 'string of pearls', the fullerenes are joined by benzene rings. The other case, called the 'bracelet', has not yet been realised and is the subject of some discussion in the literature. Possible applications of the greatest interest are polymers consisting entirely of the fullerene molecules. In contrast to crystalline fullerites, where the fullerene molecules are bound to one another (like separate layers of graphite) by the weak van der Waals forces, one would expect these polymers to have chemical bonds.

The results of the first experiments on the polymerisation of fullerenes look very promising [27, 247–256]. A polymer film of $C_{60}$ was formed [247] by ultraviolet irradiation of a fullerene film. A film prepared in this way was plastic and could be separated from the substrate. The average distance between the fullerene molecules in a film was found to be approximately 0.1 A less than the corresponding value in a fullerite crystal. In recent investigations [256] use was made of ultraviolet radiation for photoinduced polymerisation of a $C_{70}$ film. The source of this radiation was a mercury arc lamp of 300 W power. Irradiation of the film produced fullerene dimers and trimers, recorded with a mass spectrometer. Another method for the polymerisation of fullerenes involved the action of an hf gas discharge on the surface of a $C_{60}$ film containing $C_{70}$ as an impurity [248]. This produced a polymer film which had the properties of a semiconductor with a band gap of 2.1 eV at temperatures 300–500 K. The surface of the film had an amorphous structure and it contained aggregates with a diameter up to 300 A. In connection with the polymerisation of fullerenes one should mention also the recently published investigations [27] in which a film of $C_{60}$ was polymerised by bombardment with a beam of electrons of energies amounting to 3 or 1500 eV. The most important conclusion reached as a result of this investigation was that the process of polymersiation was reversible; annealing of a polymer film at $T = 470$ K for 2 h resulted in complete destruction of the chemical bonds between the fullerene molecules and recovery of the fullerite crystal structure. Successful synthesis of metallo-organic polymers of the $(C_{60}Pd)_n$, $(C_{60}Pd_2)_n$, and $(C_{60}Pd_3)_n$ type was reported in Ref. [250].

## 6. Fullerenes in solutions

### 6.1 Solubility of fullerenes

The interest in the behaviour of fullerenes in solutions is primarily due to the fact that the most common way of preparing, separating, and purifying fullerenes involves the use of solvents [54–56]. The feasibility of efficient separation of fullerenes (from soot which contains them and is formed by thermal evaporation of graphite) is due to relatively high, compared with other soot components, solubility of fullerenes in many organic compounds. The most efficient method for separating fullerenes is based on the difference between the solubilities of different fullerenes in a number of solvents, and also on the different efficiencies of extracting them from sorbents by solvents. The principles underlying the most efficient fullerene separation and purification methods are similar to those used in liquid chromatography.

Table 4 gives the results of measurements of the room-temperature solubilities of fullerenes in a number of solvents [257, 258]. It is clear from the data in this table that $C_{60}$ is practically insoluble in polar solvents such as alcohols, acetone, tetrahydrofuran, etc. This fullerene is weakly soluble in alkanes such as pentane, hexane, and decane; the solubility in alkanes increases with the number of carbon atoms. An analysis reported in Ref. [257] shows that the fullerenes are best dissolved in those solvents for which the specific enthalpy of evaporation, reduced to the specific volume of the solvent molecule, is close to the corresponding value for the $C_{60}$ molecule (approximately 100 cal cm$^{-3}$). This confirms quantitatively the old empirical rule: "like dissolves in like". The complex behaviour of fullerenes in solutions is demonstrated in particular by the data on the solubility of $C_{60}$ in decalin. It follows from these measurements that the solubility of this fullerene in normal decalin, which is a mixture of the cis and trans forms in the ratio 3 : 7, is considerably higher than the solubilities in either of these two forms.

### 6.2 Characteristic features of the behaviour of fullerenes in solutions

The very first experimental investigations of the behaviour of fullerenes in solutions have revealed their unusual properties. For example, a study of the nonlinear optical

**Table 4.** Solubility of $C_{60}$ and $C_{70}$ in various solvents at room temperature.

| Solvent | Solubility/mg ml$^{-1}$ | |
|---|---|---|
| | $C_{60}$ | $C_{70}$ |
| *Alkanes* | | |
| *n*-pentane | 0.005 [257]; 0.004 [258] | 0.002 [258] |
| cyclopentane | 0.002 [257] | |
| *n*-hexane | 0.043 [257]; 0.04 [258] | 0.013 [258] |
| *n*-decane | 0.07 [257]; 0.07 [258] | 0.053 [258] |
| dodecane | 0.091 [258] | 0.098 [258] |
| tetradecane | 0.126 [258] | |
| *m*-decalin | 4.6 [257] | |
| cis-decalin | 2.2 [257] | |
| trans-decalin | 1.3 [257] | |
| *Haloalkanes* | | |
| dichloromethane | 0.26 [257]; 0.25 [258] | 0.08 [258] |
| chloroform | 0.16 [257] | |
| tetrachloromethane | 0.32 [257]; 0.45 [258] | 0.12 [258] |
| 1,2-dibromomethane | 0.50 [257] | |
| trichloroethylene | 1.4 [257] | |
| tetrachloroethylene | 1.2 [257] | |
| dichlorofluoroethane | 0.020 [257] | |
| 1,1,2-trichlorotrifluoroethane | 0.014 [257] | |
| 1,1,2,2-tetrachloroethane | 5.3 [257] | |
| *Polar solvents* | | |
| methanol | 0.000 [257] | |
| ethanol | 0.001 [257] | |
| isopropanol | | 0.0021 [258] |
| nitromethane | 0.000 [257] | |
| nitroethane | 0.002 [257] | |
| acetone | 0.001 [257] | 0.0019 [258] |
| acetonitrile | 0.000 [257] | |
| *n*-methyl-2-pyrrolidine | 0.89 [257] | |
| *Benzenes* | | |
| benzene | 1.7 [257]; 1.44 [258] | 1.3 [258] |
| toluene | 2.8 [257]; 2.15 [258] | 1.4 [258] |
| xylene | 5.2 [257] | |
| mesitylene | 1.5 [257]; 1.0 [258] | 1.47 [258] |
| tetralin | 16 [257] | |
| o-cresol | 0.014 [257] | |
| benzonitrile | 0.41 [257] | |
| fluorobenzene | 0.59 [257] | |
| nitrobenzene | 0.80 [257] | |
| bromobenzene | 3.3 [257] | |
| anisole | 5.6 [257] | |
| chlorobenzene | 7.0 [257] | |
| 1,2-dichlorobenzene | 27 [257] | |
| 1,3-dichlorobenzene | | 36.2 [258] |
| 1,2,4-trichlorobenzene | 8.5 [257] | |
| *Naphthalenes* | | |
| 1-methylnaphthalene | 33 [257] | |
| dimethylnaphthalene | 36 [257] | |
| 1-phenylnaphthalene | 50 [257] | |
| *Other solvents* | | |
| carbon disulfide | 7.9 [257]; 5.16 [258] | 9.9 [258] |
| tetrahydrofuran | 0.000 [257] | |
| tetrahydrothiophene | 0.030 [257] | |
| 2-methylthiophene | 6.8 [257] | |
| pyridine | 0.89 [257] | |
| dioxane | 0.041 [258] | |

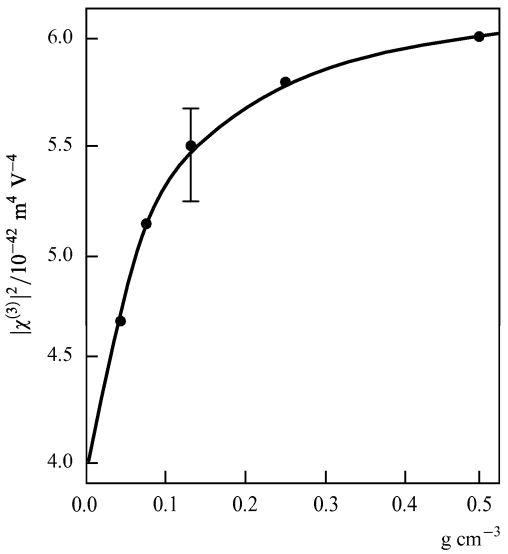


**Figure 11.** Dependence of the nonlinear third-order optical susceptibility of $C_{60}$ dissolved in benzene on the solution concentration, measured at the wavelength 1.064 μm [259].

properties of the solution of $C_{60}$ in benzene [259] demonstrated an anomalous dependence of the third-order susceptibility on the concentration of this fullerene. The results obtained with the use of a neodymium laser, emitting 1.064 μm pulses of 5 mJ energy and 50 ps duration, are presented in Fig. 11. Saturation of this dependence with increase in the solution concentration indicates the formation of aggregates consisting of a number of fullerenes. An increase in the concentration of the solution increases the average size of the aggregates and the nonlinear susceptibility of the dissolved fullerenes approaches the value reported for a fullerene crystal.

The possibility of formation of aggregates in fullerene solutions is supported also by osmometric data on the average molecular weight of $C_{60}$ dissolved in chlorobenzene and toluene [260]. The measurements were based on Raoult's law, which states that the saturated vapour pressure of a solvent containing a solute is less than the corresponding value of the pure solvent and the difference is proportional to the concentration of the solute in the solution. An analysis of the experimental results in Ref. [260] shows that the average mass of the $C_{60}$ molecules dissolved in chlorobenzene at $T = 340$ K, when the concentration of the solution by weight is about 1 g kg$^{-1}$, is approximately 30% higher than the mass of the isolated $C_{60}$ molecule. This is evidence of the formation, in a solution, of complexes consisting of at least two fullerene molecules. A similar effect does not occur in toluene solutions.

Another interesting feature of the behaviour of fullerene solutions was revealed by determination of the optical spectra representing the electronic absorption in $C_{70}$ dissolved in a mixture of acetonitrile and toluene [261]. These measurements (presented in Fig. 12) demonstrated that the nature of the spectrum depended critically on the composition of the solvent. For example, a volume concentration of acetonitrile in excess of 60% in the solvent reveals additional features of the electronic absorption in $C_{70}$, which are absent at lower acetonitrile concentrations. A strong absorption band appears in the range 550 – 800 nm, whereas the fine structure of the

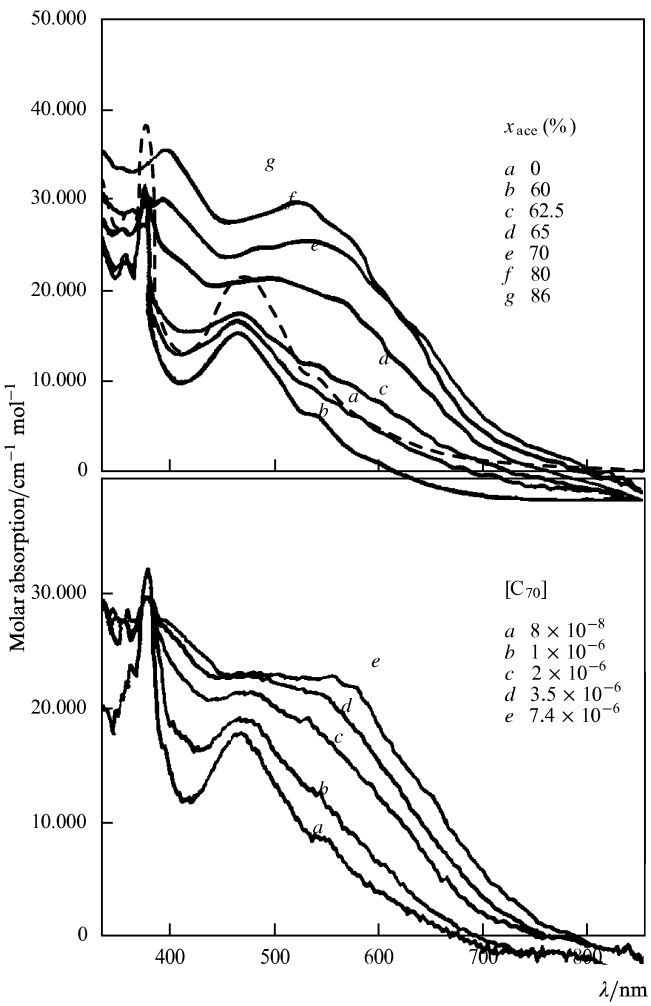


**Figure 12.** Absorption spectra of $C_{70}$, dissolved in a mixture of acetonitrile and toluene, measured for different acetonitrile concentrations $x_{ace}(A)$ in a mixture (molar concentration of fullerene $[M] = 6.6 \times 10^{-6}$) and different concentrations of the solution (B) ($x_{ace} = 70\,\%$) [261].

spectrum practically disappears at 300–400 nm. These features of the behaviour of the $C_{70}$ spectra in solutions are again attributed [261] to the possibility of formation in a solution of clusters consisting of several fullerene molecules.

The most interesting feature of the behaviour of fullerenes in solutions is related to the temperature dependence of the solubility. Fig. 13 shows the temperature dependence of the solubility of $C_{60}$ in hexane, toluene, and $CS_2$ reported by Ruoff et al. [19]. It follows from the data in this figure that the temperature dependence of the relative solubility is practically independent of the type of the solvent in a wide range of temperatures, although the absolute values of the solubility vary with the solvent by up to two orders of magnitude. An even more surprising feature is the nonmonotonic nature of the temperature dependence of the solubility of fullerenes found experimentally. The highest solubility occurs at about 280 K. A further increase in temperature is accompanied by a considerable reduction in the solubility, which falls by nearly an order of magnitude at about 400 K. This feature of the behaviour of fullerenes in solutions, like other features described above, can be explained by the formation of solution clusters containing several fullerene molecules [262, 263]. The falling nature of

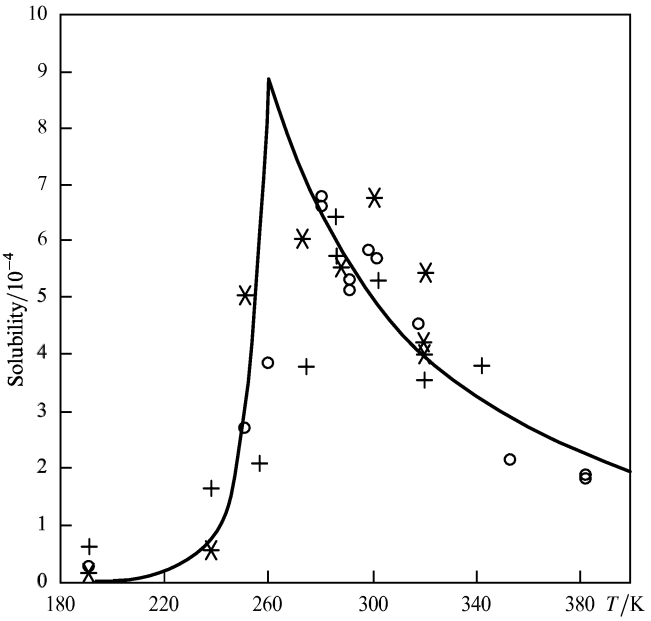


**Figure 13.** Temperature dependence of the solubility of $C_{60}$ in hexane (+, multiplied by 55), toluene (o, multiplied by 1.4), and $CS_2$ (*) [19]. The continuous curve is calculated [262] taking account of the aggregation of fullerenes in a solution.

the temperature dependence of the fullerene solubility is due to thermal dissociation of the clusters and, as a consequence of an increase in the surface of the interaction between the solute and the solvent, precipitation of a certain number of the dissolved fullerenes.

### 6.3 Cluster origin of the solubility of fullerenes

The experimental observations presented above allow us to assume that the possibility of formation, in solutions, of fullerene clusters with several molecules should influence significantly the properties of the fullerene solutions. This requires a detailed analysis of the physical factors governing the possibility of cluster formation in the fullerene solutions and a determination of the parameters of these clusters. A thermodynamic approach to this task can be found in Refs. [262, 263], where a theory of the solubility of fullerenes taking account of the possibility of cluster formation is presented. This approach is based on the drop model of a cluster, which is valid when a typical number of fullerene molecules in a cluster is $n \gg 1$. It follows from an analysis of the experimental data that this condition is satisfied reasonably in the situation represented by the nonmonotonic temperature dependence of the fullerene solubility.

Let us now consider derivation of the temperature dependence of the fullernene solubility which takes into account the possibility of the formation of clusters consisting of a certain number of fullerene molecules. It follows from the drop model of a cluster that the free energy of a cluster in a solution has two parts: the bulk (volume) part, proportional to the number of molecules $n$ in a cluster, and the surface part, proportional to $n^{2/3}$ [264, 265]. This corresponds to the assumption that the clusters consisting of $n \gg 1$ particles have the shape of a spherical drop. Hence, the function $f_n$ representing the cluster size distribution can be described by

$$f_n = g_n \exp\left(-\frac{An + Bn^{2/3}}{T}\right). \tag{7}$$

Here, the parameter $A$ is the difference between the energies of the interaction of a fullerene molecule, which is in a solid or in the bulk of a cluster, with its environment; the parameter $B$ represents a similar difference between the energies of the fullerene molecules located on the surface of a cluster; $g_n$ is the statistical weight of a cluster with $n$ particles; $T$ is the absolute temperature (the parameters $A$ and $B$ are usually expressed in terms of the absolute temperature). This form of the distribution function is based on the structural properties of the fullerene molecules. Essentially, a fullerene represents a uniform surface structure which, in contrast to planar or elongated molecules, interacts with its environment practically independently of the orientation. The large number of identical components on the fullerene surface makes it possible to represent the energy of the interaction of the molecule as a product of the specific surface interaction energy multiplied by the surface area of the molecule. This feature of the fullerene structure can be used also in the description of the interaction of clusters composed by fullerenes and a solvent. This interaction is of purely surface nature and the energy of the interaction of fullerenes with one another, both in a cluster and in a solid, is relatively low compared with the binding energies of the carbon atoms in the fullerene molecule. We can therefore assume that the specific surface energy of the interaction of the fullerene molecules with one another and with the solvent molecules is not very sensitive to the relative orientation of the fullerene molecules in a cluster.

The fullerene solubility $C$ is proportional to a sum:

$$C \propto \sum n f_n \tag{8}$$

which — subject to the condition $n \gg 1$ — can be replaced by an integral:

$$C \approx \overline{g}_n \int_1^\infty n \exp\left(-\frac{An + Bn^{2/3}}{T}\right) \mathrm{d}n. \tag{9}$$

Here, $\overline{g}_n$ is the statistical weight of a cluster, averaged over a range of values of $n$ making a certain contribution to the integral in Eqn (9). This parameter takes account of the entropy factor and it governs the absolute value of the solubility. In general, the parameter can assume various values depending on the nature of the solvent. It is naturally assumed that the dependence of $g_n$ on $n$ and $T$ is considerably weaker than the exponential function in expression (7). The parameters $A$ and $B$, the ratio of which governs the temperature dependence of the solubility, should also depend on the nature of the solvent, but the experimentally observed [19] similarity of the temperature dependences of the relative solubility of $C_{60}$ in hexane, toluene, and $CS_2$ is evidence of similar values of this ratio for the solvents in question.

We shall now consider the possibility of using Eqn (9) to describe the temperature dependences of the fullerene solubilities in nonpolar solvents presented in Fig. 13 which is taken from Ref. [19]. We can readily see that the nonmonotonic temperature dependence $C(T)$ is possible only if $B < 0$ and $A > 0$. The integral in Eqn (9), considered as a function of temperature, can then have only one extremum, which is actually a minimum. In fact, the second derivative of the function $C(T)$ is positive at the point where $\mathrm{d}C/\mathrm{d}T = 0$. It therefore follows that Eqn (9) cannot have a maximum on the temperature scale. Consequently, the formation of fullerene clusters is insufficient to account for the experimentally observed nonmonotonic temperature dependence of the fullerene solubility.

However, as pointed out in Ref. [19], the reason for the change in the nature of the temperature dependence of the solubility from rising to falling may be an orientational-disordering phase transition, which occurs in a $C_{60}$ crystal at $T = 255$ K [67]. This transition modifies the simple cubic (sc) lattice of a low-temperature $C_{60}$ crystal to the face-centred cubic (fcc) lattice, which is characterised by close packing. Moreover, this transition 'unfreezes' the rotation of the fullerene molecules about their axes. The results of experimental investigations show [67] that the transition is endothermal, that it is of the first order, and that its heat of transition is $\Delta h = 850$ K. This leads to a very different role of clusters in a fullerene solution and, consequently, to different temperature dependences of the fullerene solubility below and above the critical phase-transition temperature. In fact, at temperatures $T < T_c$, we have $A_{sc} = A_{fcc} + \Delta h$, where $A_{sc}$ and $A_{fcc}$ are the values of the parameter $A$ at temperatures below and above the critical value. This means that at $T < T_c$, the cluster size distribution function described by expression (7) falls with increase in the number $n$ much more steeply than at temperatures $T > T_c$. The low-temperature maximum of this function corresponds to $n \sim 1$, so that clusters play a relatively unimportant role in solutions at temperatures $T < T_c$. This accounts qualitatively for the rising nature of the temperature dependence of the solubility at $T < T_c$.

The temperature dependence of the solubility of $C_{60}$ in $CS_2$, calculated on the basis of the thermodynamic approach presented above (taking account of cluster formation), is compared in Fig. 13 with the experimental results of Ref. [19]. The best agreement between the calculations and experiments is obtained for the following parameters: $B = 970$ K, $A_{fcc} = 320$ K, $c_0 = 5 \times 10^{-8}$ (molar concentration of $C_{60}$). The agreement with experiment is satisfactory. One could hardly expect a better agreement because the crystal parameters, including the relative fraction of the fcc phase relative to the hexagonal close-packed (hcp) phase, depends on the method of preparation of the crystal and this can affect the results.

The validity of the drop model of a cluster used in this approach is governed by the average number $n^*$ of the fullerene molecules per one cluster. It follows from the calculations that this number rises monotonically with temperature from $n^* = 3$ at $T = 190$ K to $n^* = 11$ at $T = 260$ K. A further increase in temperature to 380 K has practically no effect on $n^*$. Therefore, condition $n \gg 1$ is obeyed in the temperature range corresponding to the fullerene solubility maximum, which justifies the use of the drop model and confirms the above hypothesis that large clusters affect the temperature dependence of the fullerene solubility.

It follows that the hypothesis of the cluster nature of the solubility of fullerenes, deduced from an analysis of recent experimental results [19, 259–261], can provide a quantitative description of the nonmonotonic temperature dependence of the solubility of $C_{60}$ in various solvents reported in Ref. [19]. The fall of the solubility with increase in temperature is observed in that range of temperatures where the existence, in a solution, of clusters consisting of a large number of fullerene molecules is thermodynamically preferred. This fall is related to the thermal dissociation of the largest clusters with rise in temperature. A further increase

in temperature should naturally increase the solubility but — as indicated by the results of calculations — for the above values of the parameters $A$ and $B$, the solubility minimum corresponds to $T \sim 4000$ K. However, at these temperatures neither solvents nor fullerenes can exist. At lower temperatures ($T < 260$ K) the role of clusters is not very important, a fact which is related to a different crystal structure of fullerene in the solid phase and is due to a higher energy of the interaction of the fullerene molecules with their environment.

It should be pointed out that this phenomenon of cluster formation in fullerene solutions had been recently confirmed by direct experiments. Measurements carried out by the light scattering method [270] demonstrated that $(C_{60})_n$ clusters form readily in a solution of fullerenes in benzene. An increase in the average cluster size continued throughout the observations (which lasted about 50 days). Light shaking of a container filled with a solution destroyed the clusters and then they started to form again. An experimentally deduced relationship between the average size of a cluster and its mass indicated that clusters had a fractal structure characterised by a fractal dimension close to 2.09. Hence, we concluded that the usual drop cluster model, employed normally in the description of the thermodynamic characteristics of fullerene clusters in solutions, is too rough and it requires considerable refinement which would take into account the fractal structure of clusters.

### 6.4 Diffusion of fullerenes in solutions

An important parameter which characterises the behaviour of fullerenes in solutions is the diffusion coefficient. The value of this coefficient determines the optimal conditions for the crystallisation of fullerenes in solutions and the possibility of their separation and purification. The measured values of the diffusion coefficient $C_{60}$ and $C_{70}$ in some solvents are listed in Table 5. It is interesting to compare the data in this table with the results of simple estimates which can be obtained from the Stokes formula describing the diffusion of spherical particles in a viscous liquid:

$$D = \frac{kT}{6\pi\eta r_s} \tag{10}$$

Here, $T$ is the absolute temperature of the liquid; $\eta$ is its viscosity; $r_s$ is the particle radius. The values of the radius $r_s$, deduced on the basis of the Stokes formula from the experimental data on the diffusion coefficient of fullerenes in various solvents, are listed in the penultimate column of Table 5. We can see that these values are considerably higher than the actual radius of the $C_{60}$ molecule, which is 3.5 A. Moreover, there is a striking difference between the values of the radius deduced for different solvents. This difference can be explained by the aggregation of fullerenes in solutions, similar to that described above. Clearly, this effect is of universal nature, although the data presented in Table 5 indicate a considerable difference of typical sizes of the fullerene clusters in different solvents.

The existence of fullerenes in solutions in the form of clusters whose average size depends on the solution concentration suggests a dependence of the diffusion coefficient of fullerenes in solutions on their concentration. In fact, at low solution concentrations, practically no clusters are formed and the diffusion coefficient is governed by the corresponding value for a single fullerene molecule.

**Table 5.** Diffusion coefficients of fullerenes in solutions.

| Solvent | Diffusion coefficient/ $10^{-6}$ am$^2$ s$^{-1}$ | $T$/K | $r_s$/Å | Ref. |
|---|---|---|---|---|
| Chlorobenzene | 3.7 ± 0.7 | 295 | 7.4 | [266] |
| 1,2-dichlorobenzene | 1.1 ± 0.2 | 295 | 7.7 | [266] |
| Pyridine | 3.1 ± 0.6 | 295 | 7.1 | [266] |
| Pyridine/acetonitrile, 9 : 1 | 3.4 ± 0.7 | 295 | 7.5 | [266] |
| Pyridine/acetonitrile, 8 : 2 | 3.8 ± 0.7 | 295 | 7.4 | [266] |
| Pyridine/acetonitrile, 6 : 4 | 4.1 ± 0.8 | 295 | 8.3 | [266] |
| Pyridine/acetonitrile, 4 : 6 | 5.1 ± 1.0 | 295 | 8.2 | [266] |
| Benzonitrile | 1.4 ± 0.3 | 295 | 12.4 | [266] |
| Dichloromethane | 4.4 ± 0.9 | 295 | 11.1 | [266] |
| Tetrahydrofuran | 1.6 ± 0.3 | 295 | 25.0 | [266] |
| Benzene | 9.1 | 298 | 4.1 | [267] |
| $CS_2$ | 18.5 | 298 | | [267] |
| $C_{70}$ in $CS_2$ | 15.6 | 298 | | [267] |
| Benzene | 8.3 ± 7 | 298 | 4.5 | [268] |

An increase in the fullerene concentration in a solution increases the average cluster size and, consequently, reduces the diffusion coefficient of the fullerene. The results of a calculation of the dependence of the diffusion coefficient of the $C_{60}$ fullerene in solutions on the concentration, carried out taking account of the formation of clusters reported in Ref. [269], are presented in Fig. 14. The thermodynamic approach, described above and based on the drop model of a cluster, was used to calculate the cluster size distribution function. It follows from the data in Fig. 14 that the diffusion coefficient of fullerenes in near-saturated solutions is approximately 30% less than the corresponding value for single molecules, due to the possibility of formation of fullerene molecular clusters in solutions.

The dependence of the diffusion coefficient of fullerenes on their concentration can be used for diffusive enrichment of a solution containing fullerenes of two types in very

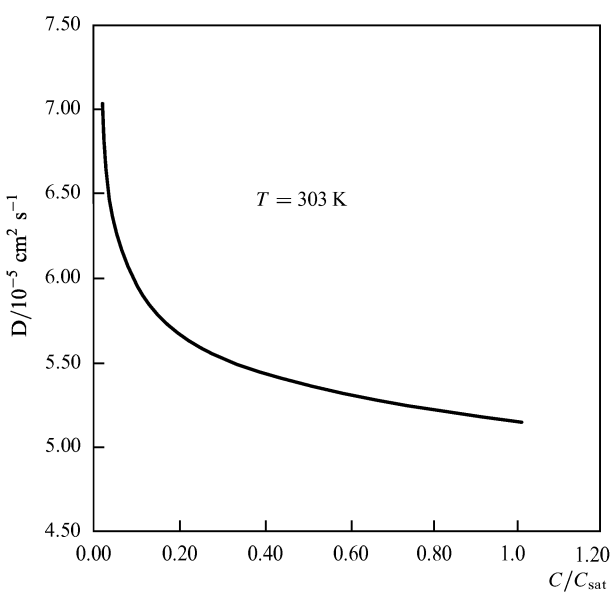


**Figure 14.** Diffusion coefficient of $C_{60}$ in toluene, calculated taking account of the formation of clusters [269].

different concentrations. In this case the fullerene representing a small amount of an impurity in a solution should have a higher diffusion coefficient than a fullerene whose concentration is close to saturation. Under transient conditions over a distance of the order of several diffusion lengths, $L_d \sim (D\tau)^{1/2}$, from a solid source of a mixture of fullerenes a significant enrichment of the solution with the fullerene present in a low concentration should take place. Here, $\tau$ is the characteristic time of the process of removal of the solution. This effect may possibly be used in the separation and purification of higher fullerenes, the concentration of which in fullerene soot is usually very low.

## 7. Fullerenes in condensed systems

### 7.1 Structure of fullerites

The solid state of bound fullerene molecules is called a fullerite. Let us consider first a fullerite consisting of the $C_{60}$ molecules. It is a typical molecular crystal in which the interaction between the carbon atoms inside the $C_{60}$ molecule is much stronger than between the atoms of the adjacent molecules. Separate $C_{60}$ molecules should be regarded as an inert species retaining its individuality in the interactions with other similar molecules. Hence, it follows that the structure of this condensed system is in many respects similar to the structure of solidified rare gases, where the structural components are again spherically symmetric atomic particles. We can therefore expect a fullerene crystal to have a close-packed structure similar to that of rare-gas crystals. In this structure [271–274] each molecule or atom has twelve nearest neighbours. There are two such structures: fcc and hcp, and the choice between them is determined by details of the interaction between the molecules, including the conditions under which a crystal is grown.

It follows from the experimental results that at relatively high temperatures a fullerene crystal consisting of the $C_{60}$ molecules can be described by the hard sphere model, which corresponds to the close-packed structures. Near room temperature both (fcc and hcp) close-packed structures are observed [6, 51, 52, 275–280], but the fcc structure is preferred. The room-temperature distance between the nearest neighbours deduced from these measurements is $1.001 \pm 0.001$ nm and the error is related to the use of different substrates on which samples are evaporated. According to the close-packed structure model, this corresponds to a density of such a fullerene crystal amounting to $\rho = 1.69$ g cm$^{-3}$.

Let us consider the close-packed structure of a fullerene crystal on the basis of the parameters of the pair interaction between the fullerene molecules. Let us do this by assuming that the diameter of the spheres is equal to the diameter of the molecules, i.e. the distance between diametrically opposite atoms in a molecule, and that the interaction potential depends on the distance between the spheres. According to the information given above, the sphere radius is 0.67 nm and the distance between the spheres is about 0.33 nm. This model applies at high temperatures when each molecule can rotate freely at its crystal lattice site. At low temperatures the structure of the surface of the $C_{60}$ molecule becomes important, so that the crystal properties depend on the anisotropy of the interaction potential, i.e. on which parts of the molecule are rotated relative to one another. In view of this, let us consider the nature of the interaction of two $C_{60}$ molecules. The interaction potential of two $C_{60}$ fullerene molecules can be constructed of two parts [326–328]. The first part is a sum of the pair interaction potentials acting between each pair of the carbon atoms belonging to different molecules. The second part is determined by the charges distributed on the surfaces of the fullerene molecules in accordance with the chemical bonds they form. In the simplest model the charge is distributed in such a way that on each of thirty midpoints of the double bonds there is a charge $-q$ and at each of the pentagon centres the charge is $5q/2$, where $0.23e < q < 0.28e$ ($e$ is the electron charge). Rotation of the fullerene molecules, which occurs at temperatures above 259 K, results in averaging of the second part of the interaction potential of the molecules, which thus vanishes, because the average charge of the molecule is zero. The parameters of the interaction potential of two fullerene molecules, averaged over the orientations of the molecules, corresponds to the equilibrium distance 10.06 A between the molecules and to the well depth 0.32 eV.

The phase transition in the $C_{60}$ fullerene crystal occurs at 257 K [12, 282, 283] and is of the first order. At high temperatures the $C_{60}$ molecules can rotate 'freely', but at low temperatures such free rotation ceases and the anisotropy of the interaction between adjacent fullerene molecules becomes significant. This produces a small change in the distance between the nearest molecules and, since the transition is abrupt, it must be of the first order. The associated change in the crystal lattice constant is relatively small. For example, according to the measurements reported in Ref. [13] and carried out by the methods of x-ray and neutron diffraction, the lattice constant changes from $1.4154 \pm 0.0003$ nm to $1.4111 \pm 0.0003$ nm (i.e. by $0.43\% \pm 0.06\%$) on transition from free to 'hindered' rotation of molecules. It should be pointed out that, in fact, the rotation of the $C_{60}$ molecules is not free at high temperatures [284]; it is hindered by the anisotropy of the molecular interaction. For example, at 283 K the period of rotation of the $C_{60}$ molecules in a crystal is $9.1 \times 10^{-12}$ s, which is only three times greater than the corresponding value for free rotation of isolated molecules [329]. At temperatures below 260 K this period changes abruptly, rising to $2 \times 10^{-9}$ s [329, 330].

This phase transition of the $C_{60}$ fullerene crystal at 257 K alters slightly the various parameters of the crystal and, therefore, can be detected by a variety of methods. These methods include x-ray diffraction [331], inelastic neutron scattering [75, 332–334], nuclear magnetic resonance [53, 281, 335], a jump in the specific heat of a crystal [336–338], Raman scattering spectroscopy [339–341], electron diffraction [342], and measurement of the positron lifetime in a crystal [285]. A combination of these results makes it possible to carry out a thorough analysis of the phase transition in question. By way of example, Fig. 15 shows the behaviour of the electric conductivity of the crystalline $C_{60}$ fullerene in the region of its phase transition.

At low temperatures, when the $C_{60}$ fullerene molecules are oriented, the crystal lattice symmetry does not match the structure of its molecules. In fact, the $C_{60}$ molecule has the $Y$ symmetry of the icosahedron, whereas the fcc lattice has the cubic symmetry, i.e. its optimal symmetry is $O_h$. Nevertheless, other lattice symmetries of the fullerene molecules are even less fitting. For example, the symmetry of the $C_{60}$ molecule could fit better the lattice with the

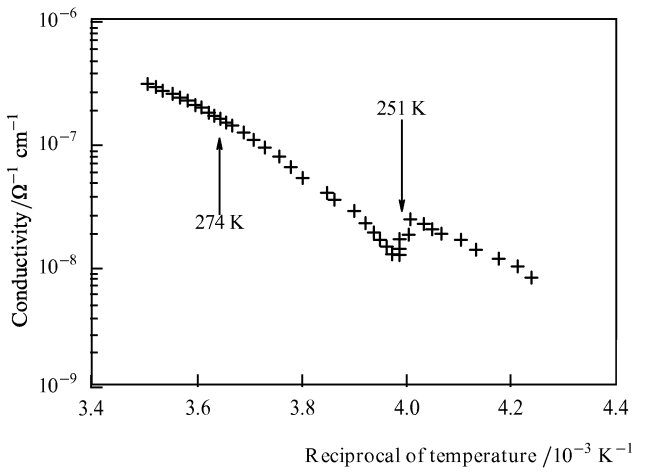


**Figure 15.** Electric conductivity of the $C_{60}$ crystalline fullerene in the region of the phase transition in the crystal [369].

icosahedral symmetry, in which each molecule would have twelve nearest neighbours, but the distance between them would not be fixed rigorously. Moreover, the molecules would then face one another with their pentagons. Such a configuration is not optimal because charges of the same sign are concentrated at the penatgon centres. The optimal configuration for the interaction between two $C_{60}$ molecules is that in which the molecules face one another with their hexagons and the centres of these hexagons are displaced by 0.09 nm relative to one another [75]. Since this cannot apply to all the molecules in a crystal, it follows that the energy per one bond in a crystal (6.1 kcal $mol^{-1}$) is somewhat lower than the maximum energy of attraction between two $C_{60}$ molecules (7.3 cal $mol^{-1}$).

We shall use current ideas to describe the properties of the crystal lattice of the $C_{60}$ fullerene at low temperatures. There are four molecules per unit cell. These molecules form a tetrahedron and the molecular orientation is repeated in each tetrahedron. These tetrahedra form their own crystal lattice which is simple cubic. This can be demonstrated by assembling the fcc lattice, formed by the fullerene molecules, in the form of four interpenetrating cubic lattices. The first term contains molecules which are at the vertices of the cubes in the fcc lattice and the other three consist of molecules located on the faces of the cubes. The other three lattices can be obtained from the first by displacing the molecules along two of the coordinates $xyz$ by an amount $a/2$, where $a$ is the lattice constant. The tetrahedron composed of the oriented molecules has one molecule from each of these lattices. Therefore, the crystal lattice formed of the tetrahedra is the simple cubic lattice. If we assume that two types of orientation of molecules in a tetrahedron are possible, we can explain the phase transition observed at 90 K [75, 343–347]. It may be that the number of such configurations of oriented molecules is larger [328]. Then the transitions between these separate configurational states may give rise to additional phase transitions. This may account for the anomalies observed at a temperature of about 160 K in the attenuation of sound [348], changes in the structural parameters [343, 346], in the permittivities [349] of a crystal, and the jumps in the specific heat [337] and in the thermal conductivity [345]. All this is evidence of a complex pattern of orientations of the $C_{60}$ molecules interacting in a crystal.

Since the symmetry of the $C_{60}$ molecules does not fit fully the symmetry of crystals with the close-packed structure, formed by the fullerene molecules, the adjacent molecules in a crystal are not oriented optimally relative to one another. This results in some instability of the structure, which is manifested by disturbance of the structure in the form of twinning. This phenomenon is associated with transitions between the hexagonal and face-centred cubic lattices. In a crystal of $C_{60}$ this is accompanied by the appearance of a number of transitional structures [350–353], which includes 'stars', polygons, etc. Disturbance of the symmetry of the fullerene crystal can also result from the nature of the growth of a crystal on a specific substrate [351, 354, 355].

The crystal structure of solid $C_{70}$ near room temperature is, as in the case of $C_{60}$, one of the close-packed structures [286, 356–360]. The coexistence of the hcp and fcc structures in a $C_{70}$ crystal depends on the nature of the substrate, on the process of formation of a crystal, and on the purity of the products used. The distance between the nearest neighbours is 10.6 A [286], which is slightly greater than the corresponding value for the $C_{60}$ crystal. In a mixed $C_{60}-C_{70}$ crystal the average distance between the adjacent molecules is 10.4 A [360].

As in the case of the $C_{60}$ crystal, at high temperatures the $C_{70}$ molecules in a crystal may alter their orientation more or less freely, whereas at low temperatures there is a definite orientation of these rotatable molecules. A phase transition occurs at about 280 K [361]. Moreover, there is a phase transition between different molecular orientations at 85 K [361]. At low temperatures the orientation of the $C_{70}$ molecules corresponds to the rhombohedral monoclinic structure [358, 361–363].

### 7.2 Electric and mechanical properties of solid fullerenes

Solid fullerenes (fullerites) are semiconductors with the band gaps 1.5–1.95 eV ($C_{60}$) [8, 94], 1.91 eV ($C_{70}$) [10], 0.5–1.7 eV ($C_{78}$) [287], and 1.2–1.7 eV ($C_{84}$) [11, 288, 289]. Investigations of electric properties of polycrystalline samples of $C_{60}$ [11, 290, 291] have revealed monotonic dependences of the resistivity on temperature and of the band gap on presure. The temperature dependence of the band gap may be due to thermal expansion of a sample, which plays the same role as a reduction in pressure [12]. These dependences may be influenced also by localised states associated with orientational disordering [11]. The increase in the band gap at pressures in excess of $2\times10^5$ bar indicates the absence of the semiconductor–metal phase transition predicted earlier [10] for pressures of $\sim2\times10^6$ bar and makes it possible to postulate the possibility of formation, at elevated temperatures, of the structure of solid carbon with covalent bonds between the carbon atoms belonging to different $C_{60}$ molecules, as in the case of diamond [11]. This hypothesis is supported in particular by the results of a recent experiment [293], according to which the $C_{60}$ solid fullerite may be transformed into new crystalline structures by high pressures (up to $5\times10^4$ bar) and high temperatures. Compression at temperatures 600–700 K leads to formation of the fcc structure with the lattice parameter $a_0 = 13.6$ A, which is 5% less than the corresponding value for the initial structure of this fullerene. Compression at temperatures 800–1100 K produces the rhombohedral structure with the hexagonal lattice parameters

$a_0 = 9.22$ A, $c_0 = 24.6$ A. This structure is characterised by much shorter average distances between the fullerene molecules in the initial crystal, so that chemical bonds form between the adjacent fullerene molecules in a crystal. These structures are metastable and slight heating (up to 600 K) at atmospheric pressure restores the initial fullerene structure.

Structural modification of crystalline fullerite under high pressures is supported also by the results of spectroscopic and x-ray investigations of samples of solid $C_{60}$ and $C_{70}$ compressed by pressures of up to $3.6 \times 10^5$ bar [292, 296]. The crystal structures formed by compression of samples are retained also when the load is removed. Then, depending on the applied pressure, one of two crystalline structures with different optical properties is formed. For example, loads of $(6-18) \times 10^4$ bar produce a crystal structure which is opaque in the near infrared and has a Raman spectrum differing from the corresponding spectrum of the starting material by wider absorption bands. Loads in excess of $1.8 \times 10^5$ bar form a crystal which is transparent in the near infrared and has mutually overlapping Raman bands. Measurements have shown that in this state a fullerite crystal is hard under the influence of twisting and that its hardness exceeds the corresponding value for diamond. The overlap of the Raman bands indicates formation of chemical bonds between adjacent fullerene molecules, i. e. it essentially indicates polymerisation of the molecular crystal. The possibility of formation of the crystal structure of diamond from polycrystalline $C_{60}$ fullerene subjected to a pressure of about $2 \times 10^5$ bar at room temperature is pointed out in Ref. [294], where the same method and apparatus were used as in the investigations cited earlier [11].

The conversion of polycrystalline graphite into diamond requires the application of a pressure of about $(3-5) \times 10^6$ bar [295].

In addition to the band gap, other important characteristics of semiconductor materials are the nature of relaxation and the relaxation time of carriers. An experimental investigation of the nature of relaxation in a $C_{60}$ fullerene film [297] shows that this process is nonexponential and the characteristic relaxation time is $\tau \sim 5 \times 10^{-8}$ s. The absence of a temperature dependence of the relaxation time in the range 150–400 K and other relationships governing the process are evidence of carrier localisation and of the hopping mechanism of recombination, including a tunnel transition of electrons between localised states.

### 7.3 New superconductors

One of the 'hot' topics in the physics of fullerenes is the existence of superconductors based on fullerenes. This topic emerged at the beginning of 1991, when it was shown that doping of $C_{60}$ solid fullerenes with small amounts of alkali metals produces a material with metallic conduction which at low temperatures goes over to the superconducting state [14, 15, 60–62, 298–301]. This material is formed as a result of treatment of films of polycrystalline $C_{60}$ fullerene in an alkali metal vapour at temperatures of several hundreds of degrees Celsius. Superconducting properties have been found for the majority of compounds of solid fullerenes formed by intercalation of alkali metal atoms into the crystal structure of $C_{60}$ in the stoichiometric ratio, either in the form of $X_3C_{60}$ or $XY_2C_{60}$ (X and Y are alkali metal atoms). Table 6 lists the parameters of superconducting compounds of this type [303]. It should be mentioned, for the sake of example, that the superconducting critical temperature of graphite intercalated with potassium is 0.55 K [302], whereas in the case of $K_3C_{60}$ it is 19 K. The critical temperature of the investigated fullerene compounds is the highest among molecular superconductors.

**Table 6.** Critical superconductivity temperature $T_c$, lattice parameter $a_0$, and fraction of the fcc structure in polycrystalline $X_3C_{60}$ or $XY_2C_{60}$ samples [304]. (Two $Na_2CsC_{60}$ samples differed from one another in respect of the preparation method.)

| Crystal | $T_c$/K | $a_0$/nm | Volume fraction of fcc (%) |
|---|---|---|---|
| $RbCs_2C_{60}$ | 33 | $1.4555 \pm 0.0007$ | 60 |
| $Rb_2CsC_{60}$ | 31 | $1.4431 \pm 0.0006$ | 60 |
| $Rb_3C_{60}$ | 29 | $1.4384 \pm 0.0010$ | 70 |
| $KRb_2C_{60}$ | 27 | $1.4323 \pm 0.0010$ | 84 |
| $K_2CsC_{60}$ | 24 | $1.4292 \pm 0.0010$ | 60 |
| $K_2RbC_{60}$ | 23 | $1.4243 \pm 0.0010$ | 75 |
| $K_3C_{60}$ | 19 | $1.4240 \pm 0.0006$ | 70 |
| $Na_2CsC_{60}$ | 12 | $1.4134 \pm 0.0006$ | 72 |
| $Li_2CsC_{60}$ | 12 | $1.4120 \pm 0.0021$ | 1 |
| $Na_2RbC_{60}$ | 2.5 | $1.4028 \pm 0.0011$ | 2 |
| $Na_2KC_{60}$ | 2.5 | $1.4025 \pm 0.0010$ | 0.1 |
| $Na_2CsC_{60}$ | 12 | | 36 |
| $Na_2CsC_{60}$ | 12 | | 6 |
| $C_{60}$ | | $1.4161 \pm 0.0009$ | |

A convenient method for the analysis of electric parameters of solid fullerenes with metallic conduction is provided by measurement of the Hall parameter. It is assumed that for each $C_{60}$ molecule in a compound of the $K_3C_{60}$ type there are three conduction-band electrons and the classical formula for the conductivity of a film $\sigma = N_e e^2 \tau / m_*$, is used; here, $N_e$ is the electron density, $m_*$ is the reduced mass of an electron, and $\tau$ is the characteristic electron scattering time. It then follows from the measurements reported in Ref. [301] that the last quantity is very small ($\tau = 3 \times 10^{-16}$ s for $K_3C_{60}$). Such a very short scattering time is explained [301] by the fine-grained structure of the investigated film, which consists of granules of 6–8 nm size. Reversal of the sign of the Hall parameter as a result of changes in temperature indicates reversal of the sign of the majority carriers, i. e. it indicates a transition from n- to p-type conduction. This transition is typical for a half-filled conduction band, which becomes completely filled in the compound $K_6C_{60}$.

Some information on the properties of the superconducting state of solid fullerenes can be obtained by investigations of the specific magnetisation of superconducting fullerene compounds. For example, the temperature dependence of the specific magnetisation of a superconducting sample of $K_3C_{60}$ [59] reveals the presence of a strong Meissner effect, confirming the superconductivity of a sample at temperatures below 18 K.

A correlation between the lattice constant $a_0$ of these compounds, which have the fcc structure, and the critical superconducting temperature [303, 304] is of fundamental importance (Fig. 16). The linear nature of the dependence is clear evidence of the role of the exchange interaction of electrons in the mechanism of the superconductivity of these

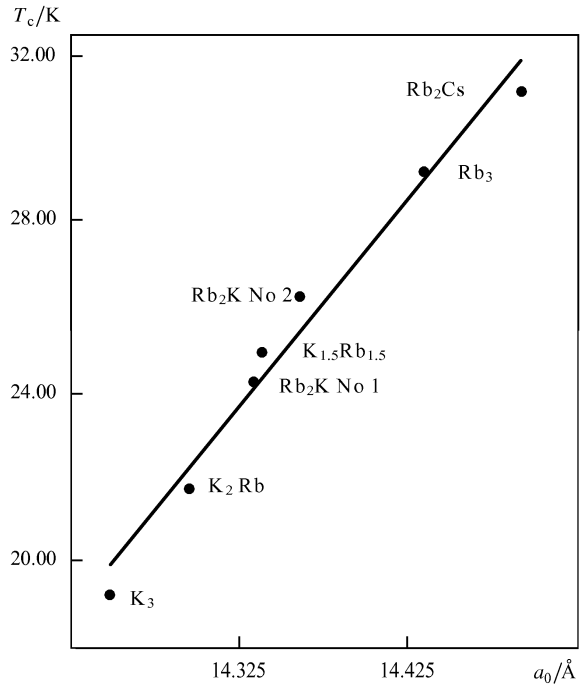


**Figure 16.** Dependence of the critical superconductivity temperature of solid fullerenes doped with alkali metal atoms on the parameter $a_0$ of the fcc crystal lattice [7, 11].

fullerene compounds. An analysis shows that, in the case of the phonon pairing mechanism, the energy of the phonons responsible for the pairing of the superconducting electrons is 300 K and the parameter representing the electron–phonon interaction resulting in electron pairing is $V \approx 0.03$ eV. The values of these quantities are independent of the nature of the intercalated atoms. This is evidence of the dominant contribution of the intramolecular vibrations of $C_{60}$ to the electron pairing energy, which governs the superconductivity parameters. It is worth noting the special role played in the superconductivity of fullerene compounds by the long-wavelength part of the phonon spectrum of $C_{60}$ solid fuller-ene [364], which reveals singularities [365]. This part of the spectrum, corresponding to intermolecular lattice vibrations with an energy of about 40 $cm^{-1}$, evidently makes a perceptible contribution to the phonon electron-pairing mechanism, which determines the appearance of superconductivity.

This correlation between the crystal lattice constant $a_0$ and the critical superconductivity temperature of alkali-metal fullerides can be used to account for the experimental dependence of this temperature on the applied pressure [305–307]. We can account for this dependence by assuming that the applied pressure alters the lattice constant and thus changes the critical superconductivity temperature. In particular, in the case of $Rb_3C_{60}$ [307], we have $dT_c/dp \approx -1$ K $kbar^{-1}$. This corresponds to $dT_c/da_0 \approx 2.36$ K $nm^{-1}$, in agreement with the value deduced from the data in Table 6.

In addition to the phonon mechanism of the formation of the Cooper pairs [308–310], mechanisms involving electrons alone have been considered [311, 312]. Some information on this point can come from the isotopic dependence of the critical temperature $T_c$. An analysis of the results of an experimental investigation of the isotopic effect in the case of the superconductor $Rb_3C_{60}$ [313] shows that the value of $T_c$ is reduced by $0.65 \pm 0.10$ K when $^{12}C$ is replaced with $^{13}C$. This represents 75% $\pm$5% of the change expected for the electron–phonon pairing mechanism. An investigation of the isotopic effect in the superconductivity of $K_3C_{60}$ [314] demonstrates a reduction in the superconducting temperature of the isotope-substituted $K_3C_{60}$ from 19.2 K to 18.8 K, which again is only a part of the change expected for the electron–phonon pairing mechanism. The superconducting temperature is practically independent of the mass of the rubidium isotope, as found [315] for samples containing pure $^{85}Rb$ and $^{87}Rb$ and also samples with a natural abundance of these isotopes (72 : 28). This has led the authors of Ref. [315] to the conclusion that the phonon–electron pairing mechanism makes only a slight contribution to the splitting energy that governs the superconductivity of the investigated material. However, the problem of the mechanism of the superconductivity of fullerene-based compounds cannot be regarded as solved and it requires further study.

The most reliable result of the investigations of the superconductivity of crystalline fullerenes doped with alkali metal atoms is therefore the correlation between the lattice constant of the fcc structure of these compounds and their critical superconducting temperature, plotted in Fig. 16. It follows from this correlation [316, 317] that replacement of one type of intracalated atom with another influences the superconductivity parameters through the change of the crystal lattice constant. This is evidently an indirect proof of the role of the electron–electron exchange interaction in superconductivity. We may assume that this relationship between the critical superconductivity temperature and the crystal lattice constant is retained also when $C_{60}$ is replaced with higher fullerenes whose crystal structure is characterised by larger values of the parameter $a_0$ [316, 317]. The critical superconductivity temperature of materials based on higher fullerenes is estimated in Refs [316, 317] by extrapolation of the linear dependence of this temperature on the lattice constant $a_0$ of the fcc structure. The postulated correspondence between the superconducting properties of the materials based on $C_{60}$ and on higher fullerenes is strongest when the fullerene molecules are nearly spherical, which corresponds to $C_{60}$. This requirement is still satisfied quite reasonably by $C_{76}$ and $C_{84}$, which — in contrast to $C_{70}$ — have similar lengths of the three main symmetry axes. The results of extrapolation of $T_c$ of superconducting materials based on the $C_{76}$ and $C_{84}$ molecules [316, 317] are presented in Table 7. We can see that, in spite of the

**Table 7.** Values of the fcc lattice constant $a_0$ and of the critical superconductivity temperature $T_c$, calculated for solid higher fullerenes doped with alkali metal atoms [18, 317].

| Material | $a_0$/Å | $T_c$/K |
|---|---|---|
| $K_3C_{76}$ | 15.12 | 62 |
| $K_2RbC_{76}$ | 15.17 | 64 |
| $K_{1.5}Rb_{1.5}C_{76}$ | 15.21 | 67 |
| $Rb_3C_{76}$ | 15.30 | 72 |
| $RB_2CsC_{76}$ | 15.37 | 76 |
| $K_3C_{84}$ | 15.54 | 84 |
| $K_2RbC_{84}$ | 15.59 | 86 |
| $K_{1.5}Rb_{1.5}C_{84}$ | 15.63 | 88 |
| $Rb_3C_{84}$ | 15.72 | 92 |
| $RB_2CsC_{84}$ | 15.79 | 96 |

relatively small difference (less than 10%) between the lattice constants of the superconducting materials based on $C_{60}$ and those based on higher fullerenes, the transition to higher fullerenes promises a considerable increase in the critical superconducting temperature. An experimental confirmation of the feasibility of high-temperature superconductivity of materials based on higher fullerenes is still lacking, which — in our opinion — is related to the difficulty of preparing pure higher fullerenes in macroscopic quantities, sufficient for superconductivity experiments. This is complicated still further by the existence of a large number of isomeric modifications of the molecules of higher fullerenes [325] and by the absence of reliable methods for the separation and purification of these modifications.

### 7.4 Optical properties of fullerene-based materials

Since fullerenes are small-gap semiconductors (in the case of $C_{60}$ fullerene single crystals the gap is 1.5 eV), they should be photoconducting when exposed to visible light. Such illumination with visible light transfers an electron to the conduction band. This is reported in Ref. [318] for a film based on polyvinyl carbazole, saturated with a mixture of the $C_{60}$ and $C_{70}$ fullerenes dissolved in toluene. The photoabsorption spectrum of the film extends over wavelengths from 280 to 680 nm and the quantum efficiency, representing the probability of formation of an electron – ion pair as a result of the absorption of one photon, is 0.9. These parameters make such a material one of the best photoconducting organics.

The $C_{60}$ fullerene is a suitable material for doubling and tripling the frequency of the incident light. This is demonstrated in Ref. [319] by measurements of the optical nonlinear third-order susceptibility for linearly polarised laser radiation with the wavelength $\lambda = 1.064$ nm. The high values of this and other nonlinear parameters are related to the nature of the processes of the absorption and emission of light by fullerenes. These values indicate that fullerenes are promising optical materials.

Experimental investigations of the nonlinear transparency of fullerene solutions and compounds [320 – 324] are revealing opportunities for the use of these solutions as optical switches or limiters of the intensity of laser radiation. This is supported by measurements reported in Ref. [320] and showing that the transparency of $C_{60}$ and $C_{70}$ solutions in methylene chloride and in toluene decreases under the influence of illumination. Illumination was provided by pulses of the second harmonic of a neodymium laser at the wavelength $\lambda = 532$ nm and of 8 ns duration. These solutions absorbed such pulses as long as their power did not exceed a certain value. For example, a solution with the transparency of 63% limited the intensity of the transmitted radiation to $\sim 10^7$ W cm$^{-2}$, whereas a solution with the transparency of 80% was characterised by an intensity threshold approximately an order of magnitude lower. Moreover, the threshold intensity for $C_{70}$ in toluene with the transparency 70% was of the same order of magnitude. The threshold intensity, which is a characteristic of an optical switch based on fullerene solutions, was several times less than the corresponding value for the materials used traditionally for such purposes (indanthrone, chloroaluminium phthalocyanine, etc.). The physical mechanism governing the operation of an optical switch based on fullerenes is related to the circumstance that the absorption of a photon with $\lambda = 532$ nm by a $C_{60}$ or $C_{70}$ molecule produces a molecule in the triplet state characterised by a photon absorption cross section several times higher than the corresponding value for the unexcited molecule. Nonlinear optical properties of fullerenes [318 – 324] may provide the basis for the development from fullerenes of special nonlinear optical components intended for the use in optical digital processors, and also for the protection of optical sensors from high-intensity radiation. All this is evidence of the promising potential applications of fullerenes as optical materials.

## 8. Conclusions

The existence of fullerenes was established in the middle eighties and an effective technology for their production was developed in 1990. The study of fullerenes is now a new and serious scientific field which is of both fundamental and applied importance. The carbon modifications represented by fullerenes have already provided a number of surprises and more can be expected also in future. This requires further study of fullerenes. Fullerenes are essentially man-made materials, the product of highly developed science and technology. Fullerenes are important not only because of new materials, technologies, and applications, but also because of new concepts which have altered somewhat our relationship to the known and well understood world.

**Acknowledgements.** We are grateful to Prof. G N Zhizhin for valuable discussions. This work was partly supported by the Russian Fund for Fundamental Research and by the Intellectual Collaboration Fund as part of the 'Fullerenes and Atomic Clusters' Programme.

## References

1. Nye J F *Physical Properties of Crystals* (Oxford: Clarendon Press, 1957)
2. Rohlfing E A, Cox D M, Kaldor A *J. Chem. Phys.* **81** 3322 (1984)
3. Kroto H W, Heath J R, O'Brien S C, Curl R F, Smalley R E *Nature (London)* **318** 162 (1985)
4. Iijima S *Nature (London)* **354** 56 (1991)
5. Ebbesen T W, Ajayan P M *Nature (London)* **358** 220 (1992)
6. Kratschmer W et al. *Nature (London)* **347** 354 (1990)
7. Haufler R E et al. *J. Phys. Chem.* **94** 8634 (1990)
8. Ajie H et al. *J. Phys. Chem.* **94** 8630 (1990)
9. Saito S, Oshiyama A *Phys. Rev. Lett.* **66** 2637 (1991)
10. Achiba Y et al. *Chem. Lett.* 1233 (1991)
11. Kikuchi K et al. *Chem. Lett.* 1607 (1991)
12. Heiney P A et al. *Phys. Rev. Lett.* **66** 2911 (1991)
13. Heiney P A et al. *Phys. Rev. B* **45** 4544 (1992)
14. Haddon R C et al. *Nature (London)* **350** 320 (1991)
15. Hebard A F et al. *Nature (London)* **350** 600 (1991)
16. Zhou O et al. *Science* **255** 833 (1992)
17. Fleming R M et al. *Nature (London)* **352** 787 (1991)
18. Bezmel'nitsyn V N, Eletskii A V *Sverkhprovodimost'* **6** 437 (1993) [*Superconductivity* **6** 343 (1993)]
19. Ruoff R S et al *Nature (London)* **362** 140 (1993)
20. Tutt L W, Kost A *Nature (London)* **356** 225 (1992)
21. *Sci. News* **16** 310 (Nov. 1990)
22. Regueiro M N et al. *Nature (London)* **355** 237 (1992)
23. Slanina Z et al. *J. Mol. Struct. Theochem.* **61** 169 (1989)
24. Bocquillon G et al. *J. Phys. Chem.* **97** 12 924 (1993)
25. Hirai H et al. *Appl. Phys. Lett.* **64** 1797 (1994)
26. Bhushan B, Ruan J, Gupta B K *J. Phys. D* **26** 1319 (1993)
27. Zhao Y B et al. *Appl. Phys. Lett.* **64** 577 (1994)
28. Hawkins J M et al *Acc. Chem. Res.* **25** 150 (1992)

29. Guo B C et al. *J. Chem. Phys.* **97** 5243 (1992)
30. Bethune D S et al. *Nature (London)* **366** 123 (1993)
31. Ebbesen T et al. *Chem. Phys. Lett.* **209** 83 (1992)
32. Iijima S, Ichihashi T *Nature (London)* **363** 603 (1993)
33. Bethune D S et al. *Nature (London)* **363** 605 (1993)
34. Ajayan P M, Iijima S *Nature (London)* **361** 333 (1993)
35. Tsang S C, Harris P J F, Green M L H *Nature (London)* **362** 520 (1993)
36. Ajayan P M et al. *Nature (London)* **362** 522 (1993)
37. Eletskii A V *Usp. Fiz. Nauk* **164** 1007 (1994) [*Phys.-Usp.* **37** 927 (1994)]
38. Osawa E *Kogaku* **25** 854 (1970)
39. Ioshida Z, Osawa E *Aromaticity (Kyoto)*, Jap. (1971)
40. Bochvar D A, Gal'pern E G *Dokl. Akad. Nauk SSSR* **209** 610 (1973)
41. Stankevich I V, Nikerov M V, Bochnar D A *Usp. Khim.* **53** 1101 (1984) [*Russ. Chem. Rev.* **53** 640 (1984)]
42. Davidson R A *Theor. Chim. Acta* **58** 193 (1984)
43. Haymet A D J *J. Am. Chem. Soc.* **108** 319 (1986)
44. Kroto H W *Science* **242** 1139 (1988)
45. Zhang Q L et al. *J. Phys. Chem.* **90** 525 (1986)
46. Kaldor A et al. *Z. Phys. D* **3** 195 (1986)
47. O'Keefe A, Ross M M, Baronavski A P *Chem. Phys. Lett.* **130** 17 (1986)
48. Hahn M Y et al. *Chem. Phys. Lett.* **130** 12 (1986)
49. O'Brien S C et al. *Chem. Phys. Lett.* **132** 99 (1986); *J. Chem. Phys.* **88** 220 (1988)
50. Cox D M, Reichmann K C, Kaldor A *J. Am. Chem. Soc.* **110** 1588 (1988)
51. Bethune D S et al. *Chem. Phys. Lett.* **174** 219 (1990)
52. Meijer G, Bethune D S *J. Chem. Phys.* **93** 7800 (1990)
53. Johnson R D, Meijer G, Bethune D S *J. Am. Chem. Soc.* **112** 8983 (1990)
54. Kratschmer W, Fostiropoulos K, Huffman D R *Chem. Phys. Lett.* **170** 167 (1990)
55. Kratschmer W, Fostiropoulos K, Huffman D R, in *Dusty Objects in the Universe* (Eds E Bussolettu, A A Cittone) (Dordrecht, Netherlands: Kluwer Academic, 1990) p. 89
56. Taylor R et al. *J. Chem. Soc. Chem. Commun.* 1423 (1990)
57. Kroto H W, in *Polycyclic Aromatic Hydrocarbons in the Galaxy* (Eds A Leger et al.) (Dordrecht, Netherlands: Reidel, 1987)
58. Foing B H, Ehrenfreund P *Nature (London)* **369** 296 (1994)
59. Maier J P *Nature (London)* **370** 423 (1994)
60. Holczer K et al. *Science* **252** 1154 (1991)
61. Rosseinsky M J et al. *Phys. Rev. Lett.* **66** 2830 (1991)
62. Wang H H et al. *Inorg. Chem.* **30** 2838 (1991)
63. Kumar V, Martin T P, Tosatti E (Eds) *Clusters and Fullerenes* (Singapore: World Scientific, 1993)
64. Smalley R E *Acc. Chem. Res.* **25** 98 (1992)
65. Kroto H W, Allaf A W, Balm S P *Chem. Rev.* **91** 1213 (1991)
66. Curl R F, Smalley R E *Sci. Am.* **265** (4) 32 (Oct. 1991)
67. Hebard A F *Annu. Rev. Mater. Sci.* **23** 159 (1993)
68. Eletskii A V, Smirnov B M *Usp. Fiz. Nauk* **161** (7) 173 (1991) [*Sov. Phys. Usp.* **34** 616 (1991)]
69. Eletskii A V, Smirnov B M *Usp. Fiz. Nauk* **163** 33 (1993) [*Sov. Phys. Usp.* **36** (1993)]
70. Flint E E *Nachala Kristallografii* (Fundamentals of Crystallography) (Moscow: Vysshaya Shkola, 1961)
71. Mackay A L *Acta Crystallogr.* **15** 916 (1962)
72. Echt O, Sattler K, Recknagel E *Phys. Rev. Lett.* **47** 1121 (1981)
73. Raoult B et al. *Philos. Mag.* **60** 881 (1989)
74. Veselovskii V S *Grafit* (Graphite) (Moscow: Nauka, 1960)
75. David W I F et al. *Nature (London)* **353** 147 (1991)
76. Hedberg K et al. *Science* **254** 410 (1991)
77. Hawkins J M et al. *Science* **252** 312 (1991)
78. Muller E Q, Tsong T T *Field Ion Microscopy: Principles and Applications* (New York: American Elsevier, 1969)
79. Tsong T T *Surf. Sci.* **70** 211 (1978)
80. Ohmae N, Tagawa M, Umeno M *J. Phys. Chem.* **97** 11 366 (1993)
81. McKenzie D R et al. *Nature (London)* **355** 622 (1992)
82. Ettl R et al. *Nature (London)* **353** 149 (1991)
83. von Helden G et al. *J. Chem. Phys.* **95** 3835 (1991)
84. von Helden G, Gotts N G, Bowers M T *Nature (London)* **363** 60 (1993)
85. von Helden G et al. *Chem. Phys. Lett.* **204** 15 (1993)
86. von Helden G et al. *Science* **259** 1300 (1993)
87. Guo B C, Kerns K P, Castleman A W Jr *Science* **255** 1411 (1992)
88. Guo B C et al. *Science* **256** 515 (1992)
89. Wei et al. *J. Phys. Chem.* **96** 4166 (1992)
90. Castleman A W Jr *Z. Phys. D* **26** 159 (1993)
91. Reddy B V, Khanna S N, Jena P *Science* **258** 1640 (1992)
92. Rantala T T et al. *Z. Phys. D* **26** 255 (1993)
93. Weaver J H et al. *Phys. Rev. Lett.* **66** 1741 (1991)
94. Saito S, Oshiyama A *Phys. Rev. Lett.* **66** 2637 (1991)
95. Xu Z-D et al. *Chin. Sci. Bull.* **39** 1347 (1994)
96. Gu Zhennan et al. *J. Phys. Chem.* **95** 9615 (1991)
97. Pradeep T, Rao C N R *Mater. Res. Bull.* **26** 1101 (1991)
98. Hare J P, Kroto H W, Taylor R *Chem. Phys. Lett.* **177** 394 (1991)
99. Diederich F et al. *Science* **252** 548 (1991)
100. Khemani K S, Prato M, Wudl F *J. Org. Chem.* **57** 3254 (1992)
101. Chatterjee K et al. *J. Org. Chem.* **57** 3253 (1992)
102. Modak D K et al. *Indian J. Phys. A* **67** 307 (1993)
103. Dance I G et al. *J. Phys. Chem.* **95** 8425 (1991)
104. Brooks J D, Taylor G H *Carbon* **3** 185 (1965); *Nature (London)* **206** 697 (1965); in *Chemistry and Physics of Carbon* (Ed. P L Walker Jr) Vol. 4 (New York: Dekker, 1968) p. 243
105. Taylor R et al. *Nature (London)* **366** 726 (1993)
106. Cox D M et al., in *Fullerenes* (Eds G S Hummond, V J Kuck; ACS Symposium Series Vol. 481) (Washington, DC: American Chemical Society, 1992) p. 117
107. Malhotra R, in *Fullerenes* (Eds G S Hummond, V J Kuck; ACS Symposium Series Vol. 481) (Washington, DC: American Chemical Society, 1992) p. 127
108. Huffman D R Phys. Today **44** (11) 22 (1991)
109. Denisov V N et al. *Zh. Eksp. Teor. Fiz.* **102** 300 (1992) [Sov. Phys. JETP **75** 158 (1992)]
110. Weeks D E, Harter W G *J. Chem. Phys.* **90** 4744 (1989)
111. Stanton R E, Newton M D *J. Phys. Chem.* **92** 2141 (1988)
112. Cyvin S J et al. *Chem. Phys. Lett.* **143** 377 (1988)
113. Wu Z C, Jelski D A, George T F *Chem. Phys. Lett.* **137** 291 (1987)
114. Cappelletti R L et al. *Phys. Rev. Lett.* **66** 3261 (1991)
115. Prassides K et al. *Chem. Phys. Lett.* **187** 455 (1991)
116. Coulombeau C et al. *J. Phys. Chem.* **96** 22 (1992)
117. Negri F, Orlandi G, Zerbetto F *Chem. Phys. Lett.* **144** 31 (1988)
118. Bethune D S et al. *Chem. Phys. Lett.* **179** 181 (1991)
119. Achiba Y et al. *J. Phys. Chem.* **98** 7933 (1994)
120. Saito Y et al. *Chem. Phys. Lett.* **204** 277 (1993)
121. Kiang C-H et al. *J. Phys. Chem.* **98** 6612 (1994)
122. Imamura M et al. *Jpn. J. Appl. Phys. Pt. 2* **33** L1016 (1994)
123. Huira H et al. *Nature (London)* **367** 348 (1994)
124. Saito Y et al. *Phys. Rev. B* **48** 1907 (1993)
125. Ruoff R S et al. *Nature (London)* **364** 514 (1993)
126. Mintmire J W, Dunlap B I, White C T *Phys. Rev. Lett.* **68** 631 (1992)
127. Hamada N, Sawada S I, Oshiyama A *Phys. Rev. Lett.* **68** 1579 (1992)
128. Saito R, Fujita M, Dresselhaus G, Dresselhaus M S *Appl. Phys. Lett.* **60** 2204 (1992)
129. Yi J Y, Bernholc J *Phys. Rev. B* **47** 1708 (1993)
130. Ebbesen T W et al. *Nature (London)* **367** 519 (1994)
131. Ruoff R S et al. *Science* **259** 346 (1993)
132. Subramoney S et al. *Nature (London)* **366** 637 (1993)
133. Tsang S C et al. *Nature (London)* **372** 159 (1994)
134. Pederson M R, Broughton J Q *Phys. Rev. Lett.* **69** 2689 (1992)
135. Heath J R et al. *J. Am. Chem. Soc.* **107** 7779 (1985)
136. Cox D M et al. *J. Am. Chem. Soc.* **108** 2457 (1986)
137. Roth L M et al. *J. Am. Chem. Soc.* **113** 6298 (1991)
138. Kikuchi K et al. *J. Am. Chem. Soc.* **116** 9367 (1994)
139. Chai Y et al. *J. Phys. Chem.* **95** 7654 (1991)
140. Johnson R D et al. *Nature (London)* **355** 239 (1992)
141. Yannoni C S et al. *Science* **256** 1191 (1992)

142. Hoinkis M et al. *Chem. Phys. Lett.* **198** 461 (1992)
143. Yannoni C S et al. *Synth. Met.* **59** 279 (1993)
144. Yoshie K et al. *Appl. Phys. Lett.* **61** 2782 (1992)
145. Pradeep T et al. *J. Am. Chem. Soc.* **114** 2272 (1992)
146. Pradeep T et al. *Indian J. Chem. A* **31** 000 (1992)
147. Bandow S et al. *J. Phys. Chem.* **97** 6101 (1993)
148. Gillan E G et al. *J. Phys. Chem.* **96** 6869 (1992)
149. Weaver J H et al. *Chem. Phys. Lett.* **190** 460 (1992)
150. Guo T et al. *Science* **257** 1661 (1992)
151. Saunders M et al. *Science* **259** 1428 (1993)
152. Christian J J, Wan Z, Anderson S L *Chem. Phys. Lett.* **199** 373 (1992)
153. Christian J J, Wan Z, Anderson S L *J. Phys. Chem.* **96** 10 597 (1992)
154. Moro L et al. *J. Phys. Chem.* **97** 6801 (1993)
155. Kikuchi K *185th Meeting of Electrochemical Society, San Francisco, 1994* Rep. 1363
156. Shinohara H N et al. *185th Meeting of Electrochemical Society, San Francisco, 1994* Rep. 1371
157. Alvarez M et al. *J. Phys. Chem.* **95** 10 561 (1991)
158. Suzuki S et al. *J. Phys. Chem.* **96** 7159 (1992)
159. Ross M M et al. *J. Phys. Chem.* **96** 5231 (1992)
160. Bandow S et al. *J. Phys. Chem.* **96** 9609 (1992)
161. Shinohara H et al. *Nature (London)* **357** 52 (1992)
162. Shinohara H et al. *J. Phys. Chem.* **96** 3571 (1992)
163. Bandow S et al. *J. Phys. Chem.* **97** 6101 (1993)
164. Shinohara H et al. *Mater. Sci. Eng. B* **19** 25 (1993)
165. Shinohara H et al. *J. Phys. Chem.* **97** 4259 (1993)
166. Weiss F et al. *J. Am. Chem. Soc.* **110** 4465 (1988)
167. Yeretzian C et al. *Chem. Phys. Lett.* **196** 337 (1992)
168. Weiske T et al. *Angew. Chem. Int. Ed. Eng.* **30** 884 (1991)
169. Weiske T, Bohme D K, Schwarz H *J. Phys. Chem.* **95** 8451 (1991)
170. Ross M, Callahan J *J. Phys. Chem.* **95** 5720 (1991)
171. Mowrey R C, Ross M, Callahan J *J. Phys. Chem.* **96** 4755 (1992)
172. Caldwell K A et al. *J. Am. Chem. Soc.* **113** 8519 (1991)
173. Caldwell K A, Gibin D E, Gross M L *J. Am. Chem. Soc.* **114** 3743 (1992)
174. Wan Z, Christian J F, Anderson S L *J. Chem. Phys.* **96** 3344 (1992)
175. Campbell E E B et al. *Z. Phys. D* **23** 1 (1992)
176. Calahan J et al. *J. Phys. Chem.* **97** 20 (1993)
177. Christian J F, Wan Z, Anderson S L *J. Chem. Phys.* **99** 3468 (1993)
178. McElvany S W *J. Phys. Chem.* **96** 4995 (1992)
179. Soderholm L et al. *J. Phys. Chem.* **96** 7153 (1992)
180. Wang L S et al. *Z. Phys. D Suppl.* **26** 297 (1993)
181. Cioslowski J *J. Am. Chem. Soc.* **113** 4139 (1991)
182. Cioslowski J, Nanayakkara A *Phys. Rev. Lett.* **69** 2871 (1992)
183. Yoshida Y *Appl. Phys. Lett.* **64** 3048 (1994)
184. Yang S N et al. *Chem. Phys. Lett.* **139** 233 (1987)
185. Lichtenberger D L et al. *Chem. Phys. Lett.* **176** 203 (1991)
186. Tomanek D, Schluter M A *Phys. Rev. Lett.* **67** 2331 (1991)
187. Hettich R L, Compton R N, Ritchie R H *Phys. Rev. Lett.* **67** 1242 (1991)
188. Mathews C K et al. *J. Phys. Chem.* **96** 3566 (1992); Sai Baba M et al. **98** 1333 (1994)
189. Chen H S et al. *J. Phys. Chem.* **98** 1016 (1994)
190. Fischer J E, Heyney P A, Smith A B *Acc. Chem. Res.* **25** 112 (1992)
191. Averitt R D, Alford J M, Halas N J *Appl. Phys. Lett.* **65** 374 (1994)
192. Zhang B L et al. *Phys. Rev. B* **48** 11 381 (1993)
193. Kim S G, Tomanek D *Phys. Rev. Lett.* **72** 2418 (1994)
194. Radi P P et al. *J. Chem. Phys.* **88** 2809 (1988)
195. Raghavachari K, Binkley J S *J. Chem. Phys.* **87** 2191 (1987)
196. Weiss F D et al. *J. Am. Chem. Soc.* **110** 4464 (1988)
197. Radi P P et al. *Chem. Phys. Lett.* **174** 223 (1990)
198. Radi P P et al. *J. Chem. Phys.* **92** 4817 (1990)
199. Wurz P et al. *J. Appl. Phys.* **70** 6647 (1991)
200. Lykke K R, Wurz P *J. Phys. Chem.* **96** 3191 (1992)
201. Yoo R K, Ruscic B, Berkowitz J *J. Chem. Phys.* **96** 911 (1992)
202. Ben-Amotz D et al. *Chem. Phys. Lett.* **183** 149 (1991)
203. Luffer D R, Schram K H *Rapid Commun. Mass Spectrom.* **4** 555 (1990)
204. Doyle R J, Ross M M *J. Phys. Chem.* **95** 4954 (1991)
205. Christian J F, Wan Z, Anderson S L *J. Phys. Chem.* **96** 3574 (1992)
206. Beck R D et al *J. Phys. Chem.* **95** 8402 (1991)
207. McElvany S W, Ross M M *Mater. Res. Soc. Proc.* **206** 697 (1991)
208. Mowrey R C et al. *J. Phys. Chem.* **95** 7138 (1991)
209. Busmann H-G, Lill T, Hertel I V *Chem. Phys. Lett.* **187** 459 (1991)
210. Wudl F *Acc. Chem. Res.* **25** 157 (1992)
211. Haddon R C *Science* **261** 1545 (1993)
212. Taylor R *Philos. Trans. R. Soc. London Ser. A* **343** 87 (1993)
213. Abrefah J et al. *Appl. Phys. Lett.* **60** 1313 (1992)
214. Kolodney E, Tsipinyuk B, Budrevich A *J. Chem. Phys.* **100** 8542 (1994)
215. Chen H S et al. *Appl. Phys. Lett.* **59** 2956 (1991)
216. Ong J N Jr *Carbon* **2** 281 (1964)
217. Newton M D, Stanton R E *J. Am. Chem. Soc.* **108** 2469 (1986)
218. Kroll G H et al. *Chem. Phys. Lett.* **181** 112 (1991)
219. Jin C et al. *J. Phys. Chem.* **98** 4215 (1994)
220. Haufler R E et al. *J. Phys. Chem.* **94** 167 (1990)
221. Ruchardt C et al. *Angew. Chem. Int. Ed. Eng.* **32** 584 (1993)
222. Attala M I et al. *J. Phys. Chem.* **97** 6329 (1993)
223. Howard J A *Chem. Phys. Lett.* **203** 540 (1993)
224. Henderson C C, Cahill P A *Science* **259** 1885 (1992)
225. Holloway J H et al. *J. Chem. Soc. Chem. Commun.* 966 (1991)
226. Selig H et al. *J. Am. Chem. Soc.* **113** 5475 (1991)
227. Zhou F, van Berkel G J, Donovan B T *J. Am. Chem. Soc.* **116** 5485 (1994)
228. Taylor R et al. *Nature (London)* **355** 27 (1992)
229. Taylor R et al. *J. Chem. Soc. Chem. Commun.* 665 (1992)
230. Scuseria G E *Chem. Phys. Lett.* **176** 423 (1991)
231. Dunlap B I et al. *J. Phys. Chem.* **95** 5673 (1991)
232. Tuinman A A et al. *J. Phys. Chem.* **96** 7584 (1992); *J. Am. Chem. Soc.* **115** 5885 (1993)
233. Gakh A A et al. *Tetrahedron Lett.* **34** 7167 (1993)
234. Kniaz K et al. *J. Am. Chem. Soc.* **115** 6060 (1993)
235. Gakh A A, Tuinman A A, Adcock J L *J. Am. Chem. Soc.* **116** 819 (1994)
236. Tebbe F N et al. *J. Am. Chem. Soc.* **113** 9900 (1991)
237. Olah G A et al. *J. Am. Chem. Soc.* **113** 9385 (1991)
238. Tebbe F N et al. *Science* **256** 822 (1992)
239. Birkett P R et al. *Nature (London)* **357** 479 (1992)
240. Weisske T et al. *Chem. Phys. Lett.* **186** 5720 (1991)
241. Morton J R et al. *J. Phys. Chem.* **96** 3576 (1992)
242. Hawkins J M et al. *J. Org. Chem.* **55** 6520 (1990)
243. Morosin B, Henderson C, Schrieber J E *Appl. Phys. A* **59** 179 (1994)
244. Fagan P J, Calabrese J C, Malone B *Acc. Chem. Res.* **25** 134 (1994)
245. Fagan P J, Calabrese J C, Malone B *Science* **252** 1160 (1991); *J. Am. Chem. Soc.* **113** 9408 (1991)
246. Balch A L, Catalano V J, Lee J W *Inorg. Chem.* **30** 3960 (1991)
247. Rao A M et al. *Science* **259** 955 (1993)
248. Takahashi N et al. *J. Appl. Phys.* **74** 5790 (1993)
249. Stephens P W et al. *Nature (London)* **370** 636 (1994)
250. Lindoy L F *Nature (London)* **357** 443 (1992)
251. Zhou P et al. *Appl. Phys. Lett.* **60** 2871 (1992)
252. Cornett D S et al. *J. Phys. Chem.* **97** 5036 (1993)
253. Zhou P et al. *Chem. Phys. Lett.* **211** 337 (1993)
254. Wang Y et al. *Chem. Phys. Lett.* **211** 341 (1993)
255. Ito A, Monkava T, Tokahashi T *Chem. Phys. Lett.* **211** 413 (1993)
256. Rao A M et al. *Chem. Phys. Lett.* **224** 106 (1994)
257. Ruoff R S et al. *J. Phys. Chem.* **97** 3379 (1993)
258. Sivaraman N et al. *185th Meeting of Electrochemical Society, San Francisco, 1994* Rep. 1211
259. Blau W J et al. *Phys. Rev. Lett.* **67** 1423 (1991)

260. Honeychuck R V, Cruger T W, Milliken J *J. Am. Chem. Soc.* **115** 3034 (1993)
261. Sun Y-P, Bunker C E *Nature (London)* **365** 398 (1993)
262. Bezmelnitsin V N, Eletskii A V, Stepanov E V *J. Phys. Chem.* **98** 6665 (1994)
263. Bezmel'nitsyn V N, Eletskii A V, Stepanov E V *Zh. Fiz. Khim.* **69** 735 (1995) [*Russ. J. Phys. Chem.* **69** 000 (1995)]
264. Frenkel' J *Kinetic Theory of Liquids* (Oxford: Oxford University Press, 1946)
265. Smirnov B M *Usp. Fiz. Nauk* **162** (1) 119 (1992); **163** (10) 29 (1993) [*Sov. Phys. Usp.* **35** 37 (1992); **36** 933 (1993)]
266. Dubois D et al. *J. Phys. Chem.* **96** 7137 (1992)
267. Hasemeyer R et al. *Ber. Bunsenges. Phys. Chem.* **98** 878 (1994)
268. Kato T, Kikuchi K, Achiba Y *J. Phys. Chem.* **97** 10 251 (1993)
269. Bezmel'nitsyn V N et al. *Khim. Fiz.* **12** 156 (1994)
270. Ying Q, Marecek J, Chu B *Chem. Phys. Lett.* **219** 214 (1994)
271. Kittel C *Introduction to Solid State Physics* 6th edition (New York: Wiley, 1986)
272. Leibfried G "Gittertheorie der mechanischen und thermischen Eigenschaften der Kristalle" in *Handbuch der Physik* (Ed. S Flugge) Vol. 7, Part 1 (Berlin: Springer, 1955) pp 104–324
273. Bunn C W *Crystals: Their Role in Nature and in Science* (New York: Academic Press, 1964)
274. Ashcroft N W, Mermin N D *Solid State Physics* (New York: Holt, Rinehart, and Winston, 1976)
275. Guo Y, Karasawa N, Goddard W A *Nature (London)* **351** 464 (1991)
276. Dravid V P, Liu S, Kappes M M *Chem. Phys. Lett.* **185** 75 (1991)
277. Schmicker D et al. *Phys. Rev. B* **44** 10 995 (1991)
278. Saito Y et al, *Jpn. J. Appl. Phys. 2* **30** L2 857 (1991)
279. Li J Q et al. *Appl. Phys. Lett.* **59** 3108 (1991)
280. Ichihashi T et al. *Chem. Phys. Lett.* **190** 179 (1992)
281. Taylor R et al. *J. Chem. Soc. Chem. Commun.* 1423 (1992)
282. Denisov V N et al. *Proceedings of First Italian Workshop on Fullerenes: Status and Perspectives, Bologna, 1992* (Eds C Taliani, G Ruani, R Zamboni) (Singapore: World Scientific, 1992) p. 65
283. Tse J S, Klug D D, Wilkinson D A, Handa Y P *Chem. Phys. Lett.* **183** 387 (1991)
284. Saito R, Dresselhaus G, Dresselhaus M S *Phys. Rev. B* **50** 5680 (1994)
285. Kristiak J, Kristiakova K, Sausa O *Phys. Rev. B* **50** 2792 (1994)
286. Vaughan G B M et al. *Science* **254** 1350 (1991)
287. Wang L S et al. *Z. Phys. D Suppl.* **26** 264 (1993)
288. Kuzuo R et al. *Phys. Rev. B* **49** 5054 (1994)
289. Ambrasser I M et al. *Phys. Rev. B* **50** 4933 (1994)
290. Duclos S J et al. *Nature (London)* **351** 380 (1991)
291. Regueiro M N et al. *Nature (London)* **354** 289 (1991)
292. Blank E et al. *Europhys. Lett.* **27** 359 (1994)
293. Iwasa Y et al. *Science* **264** 1570 (1994)
294. Regueiro M N et al. *Nature (London)* **355** 237 (1992)
295. Ball P *Nature (London)* **355** 205 (1992)
296. Blank V et al. *Phys. Lett. A* **188** 281 (1994)
297. Cheville R A, Halas N J *Phys. Rev. B* **45** 4548 (1992)
298. Sparn G et al. *Phys. Rev. Lett.* **68** 1228 (1992)
299. Haddon R C *Acc. Chem. Revs.* **25** 127 (1992)
300. Palstra T T M et al. *Phys. Rev. B* **50** 3462 (1994)
301. Palstra T T M et al. *Phys. Rev. Lett.* **68** 1054 (1992)
302. Hannay N B et al. *Phys. Rev. Lett.* **14** 225 (1965)
303. Tanigaki K et al. *Nature (London)* **352** 222 (1991)
304. Tanigaki K et al. *Nature (London)* **356** 419 (1992)
305. Mizuki J et al. *Phys. Rev. B* **50** 3466 (1994)
306. Sparn G et al. *Science* **252** 1829 (1991)
307. Fischer J E et al. *Science* **262** 1288 (1991)
308. Varma C M, Zaanen J, Raghavachari K *Science* **254** 989 (1991)
309. Schluter M A et al. *Phys. Rev. Lett.* **68** 526 (1992)
310. Zhang F C, Ogata M, Rice T M *Phys. Rev. Lett.* **67** 3452 (1991)
311. Chakravarty S, Kivelson G, Gelfand M P *Science* **254** 970 (1991)
312. Baskaran G, Tossati E *Curr. Sci.* **61** 33 (1991)
313. Ramirez A P et al. *Phys. Rev. Lett.* **68** 1058 (1992)
314. Chen C-C, Lieber C M *J. Am. Chem. Soc.* **114** 3141 (1992)
315. Burk B et al. *Phys. Rev. Lett.* **72** 3706 (1994)
316. Bezmel'nitsyn V N, Eletskii A V *Sverkhprovodimost'* **6** 437 (1993) [*Superconductivity* **6** 343 (1993)]
317. Bezmelnitsyn V N, Eletskii A V *Proceedings of Symposium on Recent Advances in the Chemistry and Physics of Fullerenes and Related Materials, San Francisco, 1994* (Eds K M Kadish, R S Ruoff) p. 1533
318. Wang Y *Nature (London)* **356** 585 (1992)
319. Hoshi H et al. *Jpn. J. Appl. Phys. 2* **30** L1 397 (1991)
320. Tutt L W, Kost A *Nature (London)* **356** 225 (1992)
321. Joshi M P et al. *Appl. Phys. Lett.* **62** 1763 (1993)
322. McLean D J et al. *Opt. Lett.* **18** 858 (1993)
323. Kost A et al. *Opt. Lett.* **18** 334 (1993)
324. Mishra S R et al. *J. Phys. B* **27** L157 (1994)
325. Wang X Q et al. *Z. Phys. D Suppl.* **26** 264 (1993)
326. Cheng A Klein M L *J. Phys. Chem.* **95** 6750 (1991); *Phys. Rev. B* **45** 1889 (1992)
327. Girifalco L A *J. Phys. Chem.* **95** 5370 (1992); **96** 858 (1992)
328. Burgos E, Halac E, Bonadeo H *Phys. Rev. B* **47** 13 903 (1993); **49** 15 544 (1994)
329. Johnson R D et al. *Science* **255** 1235 (1992)
330. Tycko R et al. *Phys. Rev. Lett.* **67** 1886 (1991)
331. Henney P A *J. Phys. Chem. Solids* **53** 1333 (1992)
332. Neumann D A et al. *Phys. Rev. Lett.* **67** 3808 (1991)
333. Pintschovius L et al. *Phys. Rev. Lett.* **69** 2662 (1992)
334. Neumann D A et al. *J. Chem. Phys.* **96** 8631 (1992)
335. Tycko R et al. *J. Phys. Chem.* **95** 518 (1991)
336. Atake T et al. *Physica C* **185** 427 (1991)
337. Matsuo T et al. *Solid State Commun.* **83** 711 (1992)
338. Grivei E et al. *Solid State Commun.* **85** 73 (1993)
339. Eklund P C et al. *J. Phys. Chem. Solids* **53** 1391 (1992)
340. Van Loosdrecht P H M et al. *Chem. Phys. Lett.* **198** 587 (1992)
341. Matus M, Kuzmany H *Appl. Phys. A* **56** 241 (1993)
342. Van Tendeloo G et al. *Ultramicroscopy* **51** 168 (1993)
343. Moret R et al. *J. Phys. I (Paris)* **2** 511 (1992)
344. Prassides K et al. *Carbon* **30** 1277 (1992)
345. Yu R C et al. *Phys. Rev. Lett.* **68** 2050 (1992)
346. David W I F et al. *Europhys. Lett.* **18** 219, 735 (1992)
347. Gudenberg F et al. *Phys. Rev. Lett.* **69** 3774 (1992)
348. Shi X D et al. *Phys. Rev. Lett.* **68** 827 (1992)
349. Alers G B et al. *Science* **257** 511 (1992)
350. Li Z G, Fagan P J *Chem. Phys. Lett.* **194** 461 (1992)
351. van de Waal B *Chem. Phys. Lett.* **202** 341 (1993)
352. Keita B et al. *Chem. Phys.* **179** 595 (1994)
353. van de Waal B W *Chem. Phys.* **187** 000 (1994)
354. van de Waal B W *Phys. Rev. Lett.* **67** 3263 (1991)
355. Harris P J F et al. *Chem. Phys. Lett.* **199** 631 (1992)
356. Chen T et al. *Phys. Rev. B* **45** 14 411 (1992)
357. Li Y Z et al. *Phys. Rev. B* **47** 10 867 (1993)
358. Vaughan G B M et al. *Chem. Phys.* **178** 599 (1933)
359. Wang X D et al. *Phys. Rev. B* **49** 14 746 (1994)
360. Fleming R M et al., in *Fullerenes* (Eds G S Hammond, V J Kuck) (Washington, DC: American Chemical Society, 1992)
361. Prassides K, in *Electronic Properties of Fullerenes* (Eds H Kuzmany, J Fink, M Mehring, S Roth) (Berlin: Springer, 1993)
362. Verheijen M A et al. *Chem. Phys.* **178** 599 (1993)
363. van Smaalen S et al. *Chem. Phys. Lett.* **223** 323 (1994)
364. Mazin I I et al. *Phys. Rev. B* **47** 538 (1993)
365. Agladze N I et al. *Opt. Spektrosk.* **76** 270 (1994) [*Opt. Spectrosc.* **76** 241 (1994)]
366. Slanina Z, Rudzinski J M, Togusi M, Osawa E *J. Mol. Struct. Theochem.* **61** 169 (1989)
367. Wakabayashi T, Kikuchi K, Shiromaru H, et al. *Z. Phys. D* **26** 258 (1993)
368. Wozawa M, Tadano A, Aogaki R, et al., in *Progress in Fullerenes* (Eds H Kuzmany et al.) (Singapore: World Scientific, 1994) p. 41
369. Peimo He, Yabo Xu, Xuejia Zhang et al. *J. Phys. Condens. Matter* **5** 7013 (1993)